RADIATION DOSE MEASUREMENT BY SODIUM IODIDE (THALLIUM) SCINTILLATION DETECTOR

By

Kebede Yacob

SUBMITTED IN PARTIAL FULFILLMENT OF THE
REQUIREMENTS FOR THE DEGREE OF
MASTER OF SCIENCE IN PHYSICS
AT
ADDIS ABABA UNIVERSITY
ADDIS ABABA, ETHIOPIA
JANUARY 2009

ADDIS ABABA UNIVERSITY

DEPARTMENT OF

PHYSICS

Supervisor: _____

Dr. Tilahun Tesfaye

Examiners: _____

Prof. A. K. Chauby

_____

ADDIS ABABA UNIVERSITY

Date: **January 2009**

Author: **Kebede Yacob**

Title: **Radiation dose measurement by Sodium Iodide (Thallium) scintillation detector**

Department: **Physics**

Degree: **M.Sc.** Convocation: **January** Year: **2008**

Permission is herewith granted to Addis Ababa University to circulate and to have copied for non-commercial purposes, at its discretion, the above title upon the request of individuals or institutions.

Signature of Author

Table of Contents

List of Figures

Abstract

Radiation dose measurement is mainly concerned with the measurement of the amount of energy absorbed in matter, when it undergoes different interaction processes with the irradiated material. The demand of radiation detectors has been increased in different fields of science and technology; some of these application areas are in the field of radiology, health-physics and personnel monitoring, in which detection instruments are demanded for the measurement of radiation dosage. The range of radiation detectors has been developed exploiting various basic methods, of which theory and technology are on a sufficiently firm basis to allow of a unified presentation. The types of radiation detectors most widely used are; Ionization chambers, Proportional and Geiger counters, and Scintillation counters. The main objective of this project work being, **" Radiation dose measurement by NaI(Tl) scintillation detector "**, we give a brief literature review of the basic processes and properties of NaI(Tl) scintillation counter in an introductory chapter, radiation interactions and interaction coefficients in chapter one, before going directly in to radiation dose measurement by NaI(Tl) detector, in chapter two part of the paper; in the effort to maintain the completeness and coherence of the discussion. However, here we are concerned only with interactions that count appreciably in reducing the intensity of incident radiation.

Acknowledgements

I would like to thank my advisor, Dr.Tilahun for his many suggestions and constant support during this projet work, specially for his guidance and providing me supportive materials to the early stages of my work.

I would also like to thank Professor A.K. Chaubey , my instructor;who expressed his interest in my work and supplied me with a knowledge, which gave me a better perspective on my own results. Fitsum Girmay, my friend, shared with me his knowledge of computer and provided many useful references and friendly encouragement. Of course, I am grateful to my wife, Emebet Kefyalew for her patience and love, without her effort this work would never have come into existence (literally).

Introduction

Radiation dose measurement is mainly concerned with the measurement of the amount of energy absorbed per unit mass of a given material, when it undergoes interaction with the irradiated material.

To do this measurement, (Absorbed dose=Energy deposited/mass): There must be a radiation source emitting a given type of radiation with a specified energy, which undergoes interactions with a given type of material, (Radiation detector), whose properties such as, mass density, atomic number...etc, suits to detect the radiation interactions that will result a measurable effect.

This measurement process cab be illustrated by the following block-diagram representing the major components involved.

The type of detectors most widely used are: Ionization chambers, Proportional and Geiger counters, and Scintillation counters. In the application areas such as in the fields of radiology, health-physics, and personnel monitoring, detection instruments are demanded for the measurement of radiation dosage.

The objective of our measurement in this project is to reach out this application through; "Radiation dose measurement by NaI(Tl) scintillation detector. "

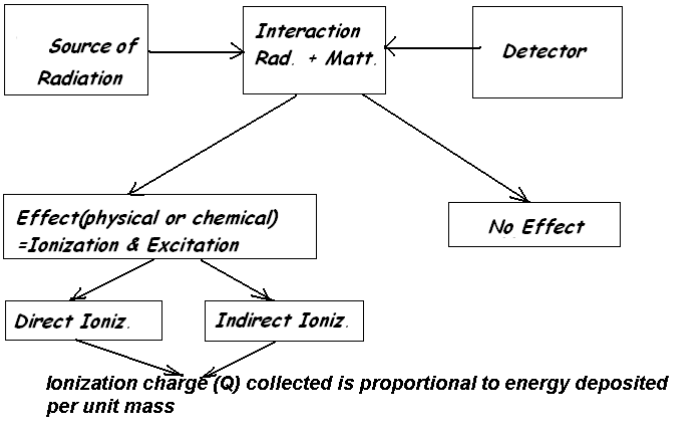

Figure 1: Block-diagram of the measurement process

Chapter 1

Properties of scintillation detectors

Before we go into the processes and properties of the detection system let's say something about the radiations of primary concern in this project paper. These radiations originate in atomic or nuclear processes, may conveniently be categorized into two general types;

1. Charged particulate radiation.
    - Fast electrons
    - Heavy charged particles
2. Uncharged radiation.
    - Electromagnetic radiation
    - Neutrons

We propose to discuss very briefly the nature of radiation which will feature very prominently in our later discussion of the scintillation counter. These are;
Fast electrons, include beta particles (positive or negative) emitted in nuclear decay,

as well as energetic electrons produced by any other process. The electromagnetic radiation of interest includes X-rays emitted in the rearrangement of election shells of atoms, and gamma-rays which originate from transitions within the nucleus itself. The energy range of interest in scientific and technological works is from 10ev to 20Mev. The lower energy bound is set by the minimum energy required to produce ionization in typical materials by the radiation or secondary products of its interaction. The radiations with energy greater than this minimum are classified as **Ionizing Radiations**. In general ionizing radiations are radiations which are capable of producing ions in matter directly, (as charged particulate radiations), or indirectly (as uncharged radiations) by virtue of their interaction with the matter concerned.

1.1 Processes in NaI(Tl) scintillation counter.

At present there are scarcely any type of radiation to the studies of which the scintillation detector has failed to make a notable contribution. Among the really striking advances which followed the general introduction of these detection instruments into atomic and nuclear physics, we must stress particularly the achievements made possible by its application to the detection and analysis of **gamma radiation**. The detection of gamma radiation generally effected by detecting the secondary charged particles (usually electrons), which they release in matter. The fundamental mechanism underlying the operation of all nuclear radiation detectors is the dissipation of energy by the charged particle in a suitable medium.

A scintillation counter involves in its operation a number of fundamental physical processes. In its elementary form takes the shape indicated in the figure below.

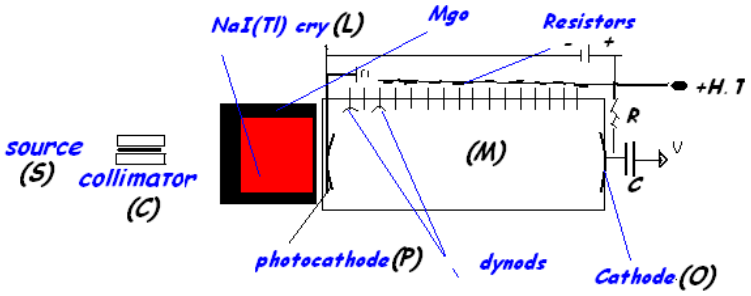

Figure 1.1: Diagrammatic representation of NaI(Tl) scintillation detector coupled with P.M. tube

A source S emits mono-energetic radiation collimated by C to fall on a luminescent material L, such as NaI(Tl). A multiplier M with a photosensitive cathode P, is usually called PM tube (photomultiplier tube), is placed so as to collect the maximum amount of light radiated by L. If M and L can not be put in good optical contact some form of light guide such as a "rod of quartz may be required. The cathode P may be semi-transparent layer of suitable photosensitive material, deposited on the end of the tube M. The electrode structure of M is the arrangement of 10 or more dynodes brought out at the end with the anode O.

The photoelectrons from P are accelerated by the applied field to the first dynode and on striking this they release secondary electrons which in turn are drawn to the second dynode and so on till a pulse of secondary electrons is finally collected at the anode O. We thus have a magnified avalanche of electrons at O for each group of one or more photoelectrons released at P. The dynode surface is so processed that about 3 to 5 slow secondary electrons are emitted by each incident fast electron. This ratio of secondary electrons to primary electrons is known as the multiplication factor per

stage, and generally between 10^7 to 10^8 gain will be achieved by the time electrons reach the last stage O.

A voltage developed across the final collector resistor R, by virtue of a current (steady or pulse) passing through it may be further amplified, if necessary by an external electronic amplifier as indicated by the arrow.

The physical processes in scintillation counting can somewhat arbitrarily be broken down into six main parts for application to spectrometry as;

1. The conversion of an incident radiation with a reasonable probability of interaction to one or more fast electrons.

2. The kinetic energy of the charged particles in the luminescent material must be converted as efficiently as possible into energy of excitation and ionization of the atoms of the scintillator.

3. The de-ionization and de-excitation of the atoms should result in the emission of fluorescent radiation (scintillation light) and this radiation should be transmitted as freely as possible through the luminescent material. The radiation should be of such wavelength as to match well with the known spectral characteristic curve of the photomultiplier.

4. Assuming the spectral distribution curve of the fluorescent radiation and the spectral sensitivity curve of the tube are well matched, the photosensitivity of the cathode of the tube should be high so that the maximum emission of photoelectrons is secured.

5. The number of fluorescent quanta emitted (and the fraction reaching the cathode) should be proportional, if possible to the energy expended by the incident radiation.

6. The number of photoelectrons released by the fluorescent quanta should in turn be directly proportional to the expended energy.

Provided these two last conditions are satisfied, and to a large extent in practice they are, the scintillation detector can be used to produce an impulsive charge at the final collector of magnitude proportional to the energy dissipated by the ionizing particle within the scintillator. Measurement of the amplitude of the output pulses thus can yield information on the energy of a homogeneous radiation. The detector is then employed as a spectrometer.

1.2 Properties of a scintillator

The ideal scintillation material should possess the following properties;

- It should convert the Kinetic Energy of charged particles into detectable light with a high scintillation efficiency.

- This conversion should be linear-the light yield should be proportional to deposited energy over as wide a range as possible.

- The medium should be transparent to the wavelength of its own emission for good light collection.

- The decay time of the induced luminescence should be short so that fast signal pulses can be generated.

- The material should be of good optical quality and subject to manufacture in sizes large enough to be of interest as a practical detector.
- Its index of refraction should be near that of glass(i.e 1.5) to permit efficient coupling of the scintillation light to a photomultiplier tube.

No material simultaneously meets all these criteria, and the choice of a particular scintillator is always a compromise among these and other factors.

The most widely applied scintillators include: the Inorganic Alkali Halide crystals, of which NaI is the favorite, and Organic based liquids and Plastics. The inorganic tend to have the best light output and linearity, but with several exceptions are relatively slow in their response time. Organic scintillators are generally faster but yield less light. The intended application also has a major influence on the choice of a scintillator. The high Z-value of the constituents and high density of inorganic crystals favor their choice for gamma-ray spectroscopy, whereas organic scintillators are often preferred for beta spectroscopy and fast neutron detection.

Since our major concern in this project work is dose measurement by Thallium activated NaI(Tl) scintillator we concentrate on the light emission properties of Inorganic Scintillators. The properties of NaI(Tl) crystal can be summarized as in the following table. [2]

Property	Value
Specific gravity	3.67
Wavelength of maximum emission(nm)λ_{max}	415
Index of refraction at λ_{max}	1.85
Principal decay constant (μs)	0.23
Pulse 10-90per rise time(μs)	0.5
Total light yield in photons/Mev	38000
Absolute scintillation efficiency for fast electrons	11.3 per
Relative gamma-ray pulse height with Bialkali PM tube	1.00

Table 1.1 Properties of NaI(Tl) scintillator

1.2.1 The basic scintillation meachanism

Inorganic Phosphors: Most of the phosphors of this type used in scintillation counters are impurity activated. Excitation of an electron into the conduction band of a phosphor crystal leaves behind an electron vacancy, a positive hole. This moves to an impurity center and ionizes it. A very short time after excitation, therefore, the phosphor contains electrons in the conduction band, and one ionized impurity center for each such electron. In a perfect crystal, each electron will drop into a center, neutralizing it, and forming an excited state for which, the transition to the ground state is allowed as shown in the figure (a) below; The center will then decay with the emission of radiation.Since this is an allowed transitions, the life time of the excited state is small. Under these conditions, the phosphor shows fluorescence with a short decay time of the order of $10^{-7} sec$. Referring to activated crystals, it is found that the emitted radiation is usually associated with the activator, although the absorption of the incident radiation occurs chiefly in the band corresponding to the host lattice.

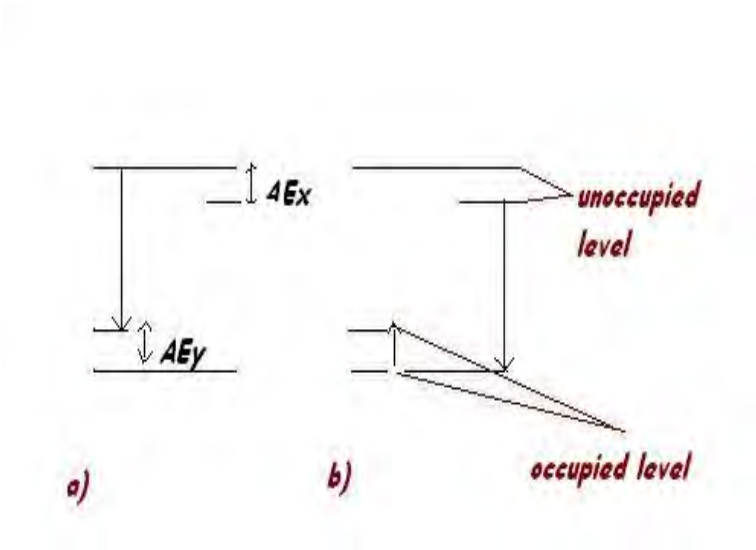

Figure 1.2: De-excitation mechanisms involving electron traps,hole traps or both

The next section will emphasizes how this absorption takes place when a gamma-ray interacts within the detector material, NaI(Tl).

Chapter 2

Radiation Interactions and Interaction Coefficients

INTRODUCTION:

One of the efficient methods of counting gamma-rays and measuring their energies is their detection by a scintillation gamma-ray spectroscopy. In order for the detector to respond at all, the radiation must undergo interactions. Since an X-ray or gamma-ray photons are uncharged and creates no direct ionization or excitation of the material through which it passes, the detection of electromagnetic radiation is, therefore, critically dependent on causing the X-ray and gamma-ray photons to undergo interactions that transfer all or part of the photon energy to an electron, and the electron in its turn deposit its energy in the detector material. Therefore, the interaction of ionizing radiation in NaI(Tl) detector can be categorized into;

- Gamma-ray interactions.
- Charged particle interactions.

2.1 Gamma-Ray Interactions

From all the interactions that the gamma ray undergoes with matter the main interaction that results in the appreciable energy deposition are the photoelectric effect, the compton effect and the pair production, which are discussed in the next sub-sections. Here we want to emphasize the contribution of each processes to the absorption of gamma-ray energy in the NaI(Tl) detector.

The basic principle is that: If the gamma-rays are allowed to produce secondary electrons in a suitable fluorescent transparent crystal, then these can be determined by measuring the light emitted from the crystal. The light originates in excited atoms produced by the secondary electrons as they are brought to rest by the collisions in the crystal.

2.1.1 The photoelectric absorption process

A gamma-ray of energy, E_γ undergoing a photoelectric effect within NaI(Tl) crystal, and will eject an electron from the atomic shells. The emitted photoelectron will have a kinetic energy, E;

$$E = E_\gamma - E_b \tag{2.1.1}$$

The binding energy per electron of the K-shell electrons is given by;

$$E_b = R(Z-1)^2 \tag{2.1.2}$$

Where R=13.5ev is the Rydberg constant and Z is the atomic number of the absorber. The binding energy per electron for the L and M-shell electrons are given by; $E_b = R(Z-5)^2/4$ and $E_b = R(Z-13)^2/9$, respectively. The outer most orbits are known as valence orbits, and excitation of electrons in these gives rise to optical spectra.

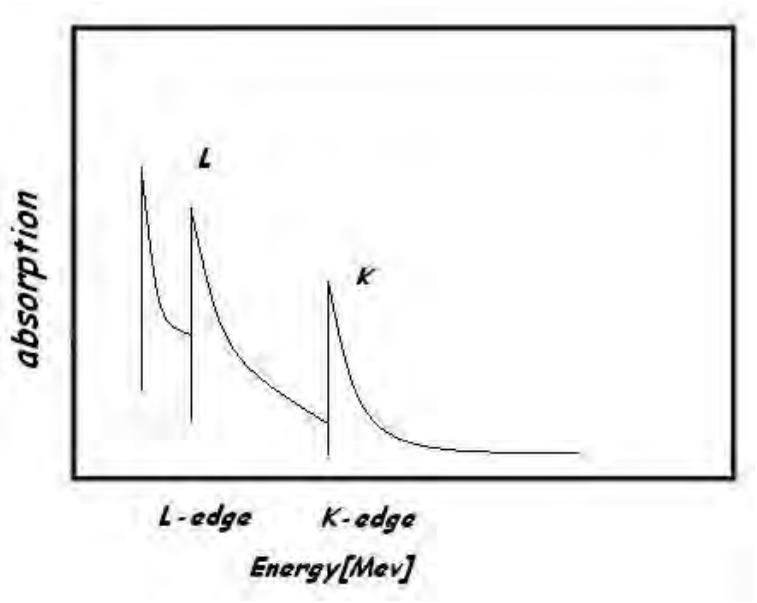

Figure 2.1: Variation of photoelectric absorption with increasing quantum energy.

Finally beyond the excitation and ionization levels we have unfilled states forming a continuum. A photon of sufficient energy may remove an electron from any of the shells and raise it to one of the bound states previously unoccupied or it may eject electron from the atom and impart to it some kinetic energy of motion, thereby leaving the atom in the ionized state.

In absorption measurements with such quanta we observe then, as the frequency ν of the radiation is increased, a series of discontinuities, as shown in the figure 2.1.

These discontinuities corresponds to the shells and sub-shells of the atomic orbits. Starting at low values of frequency(ν) the first discontinuity corresponds to the energy (hν) at which incident quanta can provide the necessary energy of several ev which will excite electrons in the optical orbits. Further increase in frequency gives rise to excitation of electrons in the more tightly bound orbits and finally, as shown

diagrammatically in the figure 2.1, the L and K shell electrons absorb the energy. The absorption edges which appear on the curve are observed at those values of h ν which corresponds to the release of electrons from the atom with zero KE. It would be useful in counting studies to have formula which would represent adequately the variation of absorption with ν over large ranges of ν values but the discontinuities prevent this. Most of the formulae that are available apply over a somewhat limited energy range and we shall refer to some of these as follows;[1]

$$\sigma_p = \frac{128\pi}{3}\left(\frac{e^2}{m_o c}\right)\left(\frac{\nu_k^3}{\nu^4}\right)\left(\frac{\exp(-4\varepsilon \cot^{-1}(\varepsilon))}{1-\exp(-2\pi\varepsilon)}\right) \tag{2.1.3}$$

Where ν_k is the frequency corresponding to the K-absorption edge. And $\nu(> \nu_k)$ is the frequency of the quanta involved, related by;

$$\varepsilon = \frac{\nu_k}{\nu - \nu_k} \tag{2.1.4}$$

A simplified formula for σ_p (photoelectric absorption cross-section) near ν_k is;

$$\sigma_p = \frac{6.31 \times 10^{-18}}{Z^2}\left(\frac{\nu_k}{\nu}\right)^{8/3} \tag{2.1.5}$$

This formula holds true for a single K-shell electron. Still more complicated treatments permit calculation of the contribution to absorption arising from excitation of the L and M shells. At quantum energies which are large compared with the energy of the K absorption edge, a frequent situation in the passage of hard gamma-ray through matter, we can neglect $(h\nu_k)$, and the differential cross-section for the ejection of photoelectrons into the elementary cone of solid angle $d\Omega = \sin\varphi d\varphi d\phi$ is given by;

$$d\sigma_p = \frac{r_o^2 Z^5 \alpha^{-7/2}}{(137)^4} 4\sqrt{2}\frac{\sin^2\varphi\cos^2\phi}{(1-\beta\cos\varphi)^4} d\Omega \tag{2.1.6}$$

Where ($r_o = \frac{e^2}{m_o c^2}$) is the classical electron radius,(1/137) is fine structure constant, $\beta = V/c$ and $\alpha = h\nu/m_o c^2$. The angles involved in the spacial distribution of photo-electrons, when the direction of incident photons is in the positive X-axis are ϕ=the azimuthal angle and φ=the longitudinal angle. When this is integrated over the angles and allowing for both K-shell electrons, we obtain the cross-section for the process in the higher energy region as;

$$\begin{aligned} \sigma_p &= \int \frac{d\sigma_p}{d\Omega} d\Omega \\ \sigma_p &= \frac{4\sqrt{2}\sigma_o Z^5 \alpha^{-7/2}}{(137)^4} \end{aligned}$$

Where $\sigma_o = \frac{8\Pi r_o^2}{3}$, is the classical cross-section for scattering. In the region of high quantum energy the relativistic wave equation yields;

$$\sigma_p = (3/2)\sigma_o \left[\frac{Z^5}{(137)^4}\right] \alpha^{-1} \tag{2.1.7}$$

Note That: the relativistic result indicates that in this region the absorption decreases more slowly with increasing photon energy.

2.1.2 The compton absorption process

Equally involved in the examination of electromagnetic radiation by counters is the compton process. This process requires quantum mechanical interpretation, but it is useful to note that the transition to this from classical scattering takes place gradually as the photon energy increased through Raman scattering. When the binding energy of the scattering electron exceed the quantum energy of the incident photons, the latter suffers classical scattering, the energy of such scattered photons being identical

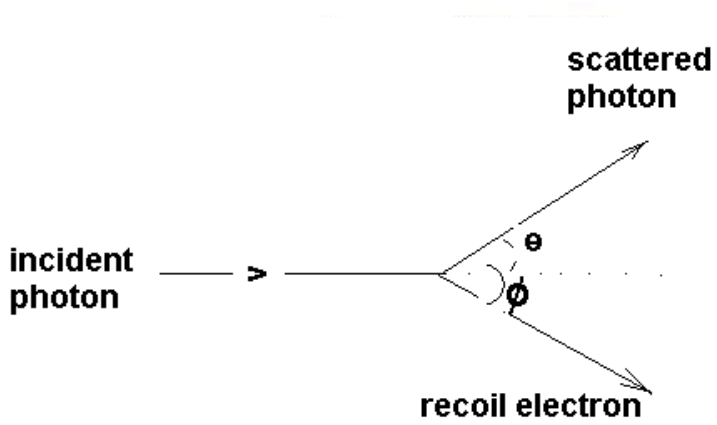

Figure 2.2: Diagram of collision between a photon and a free electro.

with that of the incident photons. When the quantum energy is sufficient to raise the electrons into the continuous spectrum, imparting to them some kinetic energy of motion, the scattered photons take the balance of available energy(apart from a very small amount which goes to the nucleus). The conservation of energy and momentum give the relations a)the energy of scattered photon b) the energy of recoil electron(compton electron) c) the change in wavelength as given below.

1. $E'_\gamma = h\nu' = \frac{h\nu}{(1+\alpha(1-\cos\theta))}$
2. $E = h\nu - h\nu' = h\nu[1 - \frac{1}{1+\alpha(1-\cos\theta)}]$
3. $\Delta\lambda = 0.0242(1-\cos\theta)\mathring{A}$

Note that except for $h\nu \ll m_o c^2$ we can neglect classical and Raman scattering and regard compton scattering as the only important scattering process.

The angular distribution of the scattered radiation is given by;

$$R^2 I_o d\Omega / I = \frac{r_o^2 d\Omega (1+\cos^2\theta)}{2\big(1+(1-\cos\theta)\big)^3}\left[1+\frac{\alpha^2(1-\cos\theta)^2}{(1+\cos^2\theta)1+\alpha(1-\cos\theta)}\right] \tag{2.1.8}$$

Where I is the scattered intensity into an element of solid angle $d\Omega$ at distance R and r_o is the classical electron radius. Hence, for the calculations of number of quanta we must multiply equation 2.1.8 by $1+\alpha(1-\cos\theta)$. Then cross-section for compton scattering after integrating equation 2.1.8 we get;

$$\sigma_{kN} = 2\pi(\frac{e^2}{m_o c^2})^2\left[\frac{(1+\alpha)}{\alpha^2}[\frac{2(1+\alpha)}{(1+2\alpha)}-\frac{\log(1+2\alpha)}{\alpha}]+\frac{\log(1+2\alpha)}{2\alpha}-\frac{(1+3\alpha)}{(1+2\alpha)^2}\right] \tag{2.1.9}$$

Which has the asymptotic forms;

- For $\alpha \ll 1$;

$$\sigma_{kN} = \sigma_T\left[1-2\alpha+(26/5)\alpha^2...\right] \tag{2.1.10}$$

- For $\alpha \gg 1$;

$$\sigma_{kN} = (3/8)\sigma_T(1/\alpha)\bigg(\log 2\alpha + 1/2...\bigg) \tag{2.1.11}$$

Where $\sigma_T = (8\Pi/3)(\frac{e^2}{m_o c^2})^2$ is classical scattering cross-section for an electron.
Two points of special importance in scintillation spectrometry emerge from the study of compton process, firstly;

- At $\theta = 90deg, E'_\gamma = \frac{h\nu}{(1+\alpha)}$
- At $\theta = 180deg, E'_\gamma = \frac{h\nu}{(1+2\alpha)}$

Hence the maximum possible energy variation in backward scattered quanta is;

$$\Delta E'_\gamma = h\nu\left[\frac{1}{(1+\alpha)}-\frac{1}{(1+2\alpha)}\right] \tag{2.1.12}$$

This indicate that the maximum energy variation in these quanta is a small fraction of hν; therefore, the forward going recoil electrons must therefore be fairly homogeneous in energy and this fact has been used to advantage in designing scintillation spectrometer of good resolving power.

Secondly we can show that at large values of hν the scattered quanta and recoil electrons tend to be with in a cone of relatively small angle and this angle decreases with increasing hν. That is, the forward tendency of the recoil electrons and the scattered quanta at high quantum energies is one of the significance in the design of large scintillation systems analyzing high energy quanta.

2.1.3 The pair-production absorption process

The process of materialization of a photon into a positive and negative electron is the most probable at energies above a few Mev, at least in high-Z materials.

At present we are chiefly interested in gamma-ray spectroscopy by scintillation methods and from this point of view it is important to know the angular distribution of the pair of electrons with respect to the direction of incidence of the materializing quantum, and with respect to each other.

A useful approximate formula is given by BETHE and HEITLER, it neglects the difference in the sign of the charges since its effect is negligible except at low energies. This formula is given by;[1]

$$N(\theta)d\theta = \frac{\theta d\theta}{(m_o c^2/W + \theta^2)^2} \tag{2.1.13}$$

Where W is the average total energy(including rest energy) of either electrons.

By differentiating the angle of maximum emission is found.

$$\theta_{max} = \frac{m_o c^2}{\sqrt{3}W} \tag{2.1.14}$$

At very high energies the term $(m_o c^2/W)$ can be neglected and $N(\theta) = 1/\theta^3$ except at very small θ. Thus in this region the electrons are emitted very close to the direction of incident photon, the intensity falling off as $1/\theta$. The cross-section for materialization into a positron and electron is nearly independent of the energy of any one of the particles though tending to peak a little at very high or low values. Analytic integration of the distribution function for pairs is possible only in the extreme relativistic case and for screening is either negligible or complete, giving the cross-section for the pair production, respectively by the following expressions.

$$\begin{aligned} \sigma_{pr} &= 4\overline{\sigma}\big[7/9\ln(\frac{2h\nu}{m_o c^2}) - 109/54\big] \\ \sigma_{pr} &= 4\overline{\sigma}\big[7/9\ln(183Z^{-1/3}) - 1/54\big] \end{aligned}$$

Where $\overline{\sigma}$ is;

$$\overline{\sigma} = (Z^2/137)(e^2/m_o c^2)^2$$

Where Z is the atomic number of the material.

2.1.4 Summary of cross-sections

COMPTON CROSS-SECTION;

The variation of scattering cross-section with the scattering angle, is described by Kelin-Nishina formula, which predicts the energy spectra for the scattered electrons. The formula is found to be valid for energy of gamma as high as 90Mev. Integration of the cross-section over θ gives the total scattering cross-section, and the cross-section

per atom, σ_c is obtained by multiplying by Z, the atomic number. Values of σ_c, thus obtained is valid over the region in which the binding energy of the electrons is small compared with energy of gamma, so that they may be considered free. It is found that the cross-section may be expressed approximately by;[10]

$$\sigma_c = (0.2E^{-1/2}Z)[barn] \tag{2.1.15}$$

PHOTOELECTRIC CROSS-SECTION:

The absorption in the outer shell of the atom contributes about 20percent to the photoelectric cross-section (σ_p) for various materials. For high value of E larger than the k absorption edge, it is given by;[3]

$$\sigma_p = 3 \times 10^{-9}E^{-7/2}Z^5[barn] \tag{2.1.16}$$

Note that for high value of gamma energy the cross-section varies as E^{-1}. The photoelectrons of energy greater than 100Kev are emitted in the forward direction.

PAIR-PRODUCTION CROSS-SECTION:

Materialization of a photon into electron-positron pair takes place in the region of an atomic nucleus, which must be present to conserve momentum.The cross-section for pair production increase rapidly from zero at 1.02Mev energy.And given approximately by;[9]

$$\sigma_{pr} = 6.2 \times 10^{-5}(E_\gamma - 1.02)^{2.1}Z^2[barn] \tag{2.1.17}$$

Note that particles produced are emitted in the forward direction, in a solid angle of the order of $(1/2E_\gamma)$. Note that: Evaluation of this spectrum by taking an absorber curve, is one of the methods of determining the gamma ray energies. The curves of fig. 2.3 show the absorption for the three processes discussed above.

The quantity usually measured, linear or mass attenuation coefficient should be

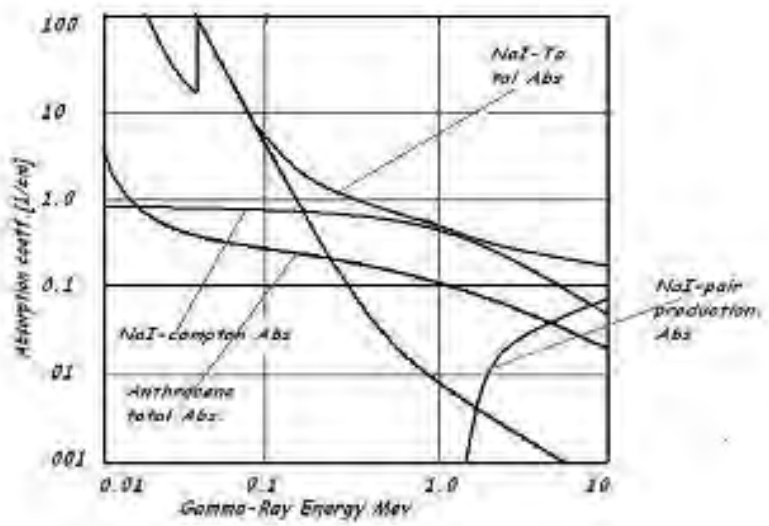

Figure 2.3: Energy dependence of various gamma-ray interaction processes in NaI(Tl)(From the atomic Nucleus by R.D Evans)

related with the concept of cross-section. If I_o is the initial intensity and I is the intensity after the beam is transmitted through a slab of thickness $\ell[cm]$, then the two intensities are related by;

$$I = I_o \exp(-\mu\ell) \tag{2.1.18}$$

Where μ is called the linear absorption coefficient. If $\rho[g/cm^3]$ is the density of the material, then the product $m = \rho\ell[g/cm^2]$ is defined as the mass thickness of the absorber. $\mu_m = \mu/\rho$ is defined as the mass absorption coefficient. Then the above relation can be written as;

$$\begin{aligned} I &= I_o \exp(-\mu(m/\rho)) \\ I &= I_o \exp(-\mu_m m) \end{aligned}$$

Suppose the cross-section for gamma-ray absorption is denoted by σ. An area of

$1cm^2$ and thickness $d\ell$ contained $(nd\ell)$ atoms, if n is the number of atoms per cm^3. Hence, an area of $(\sigma nd\ell)$ is opaque to the photons incident upon it. And if dI is the diminution intensity of a beam of intensity I, then;

$$\frac{dI}{I} = -\sigma nd\ell \tag{2.1.19}$$

Since $dI/I = -\mu d\ell$ this implies;

$$\begin{aligned} \mu_m &= \frac{n\sigma}{\rho} \\ \mu &= n\sigma \end{aligned}$$

2.2 Energy Loss Of Charged Particles

The loss of energy by charged particle in its passage through matter is caused by the interaction of the electric field of the moving charge and the electronic structure of the surrounding medium. Such interaction results in the deceleration of the particle, and the acceleration of electrons which may acquire enough energy to break loose from their parent atom.

Uncharged particles(neutrons) and electromagnetic radiation quanta(gamma rays photons) have no such continuous body of forces acting on them as they pass through a medium. Interaction, when it does occur, results in the transfer of an appreciable part, or all, of the energy to one or two charged particles. Examples of this process are the elastic collision of fast neutron with a hydrogen nucleus, which results in the projection of a proton, and the compton scattering of a gamma quantum resulting in the transfer of the energy to an electron. In such cases, the primary energy is distributed through the mediation of a secondary charged particle, and detection will take place.

2.2.1 Charged particle interactions

It is important to understand the different processes through which charged particles interact with matter because the behavior of the radiation detector ultimately depends on these interactions. In the following sections we shall consider only those charged particles(VIZ electrons, positrons, protons and alpha particles) which are encountered in nuclear spectroscopy and to incident energies of the order 0.1-5Mev, for which coulomb forces are mainly responsible for these interactions.
In describing mainly ionization, scattering and radiative energy losses caused by electromagnetic interaction it is better to divide the charged particles into two categories:

1. "light" particles; electrons and positrons

2. "heavy" particles; protons and alpha particles

such a classification is relevant because electrons interact with matter in a way different from protons or alpha particles. Thus electrons by virtue of their small mass undergo large angle of scattering and radiative collisions(bremsstrahlung). Secondly, in nuclear spectroscopy alpha particles and protons are usually mono-energetic, while electrons have a continuous distribution of energies.

2.2.2 Interaction of light charged particles with matter

- Electrons.

    1. Inelastic collision: This is inelastic collision of incident electrons with bound atomic electrons in matter and is the most important mechanism

by which incident electrons lose their energy in their passage through matter. During such inelastic collisions incident electrons transfer part of their energy to a bound atomic electrons taking the atom to an excited state or unbound state (ionization). This problem has been treated quantum mechanically and it has been shown that the mean energy loss due to inelastic collisions is given by Bethe-Bloch formula in the subsection 2.2.4 .

2. Radiative collision: Is collision of electrons with the atomic nucleus. Incident electrons passing through the field of a nucleus experience a deflection which resultants emission of radiation. This process is known as bremsstrahlung (continuous X-rays), which leads to a loss of kinetic energy of incident electron. This can be considered as a radiative type of inelastic collision between the electron with atomic nucleus. The rate of energy loss by this interaction is proportional to the square of atomic number of the target atom.

3. Elastic collision: Incident electrons can have an elastic collision with a nucleus resulting a deflection of electrons without any radiative loss. The cross-section for this process is of the order of $(\frac{e^2}{m_0 v^2})^2$. where v is velocity of incident electron and the cross-section increases with Z^2.[4]

- positron. The interaction of positron with matter is almost identical with that of electrons but with some minor differences. There is a very important way by which positrons can annihilate with electrons via the formation of (e^+e^-) hydrogen like atom called positronium. the positron annihilation leads to two photons if the electron-positron spin is anti-parallel and into three photons if

the spin orientation is parallel.

2.2.3 Interaction of heavy charged particles

Heavy charged particles like protons and alpha particles lose their energy mostly by ionizing the atoms of the material they pass through. During its passage the heavy charged particle give up its energy to the atoms of the absorber through an electromagnetic interaction. The electrons of the absorber atom either get excited or leave the atom depending on the energy gained by it. Both these processes will be called as the ionization of the atom. Elastic scattering of alpha particles by nuclei or bremsstrahlung loss is negligible at the energies which we are considering.

While considering the energy loss of protons and alpha particles it is convenient to speak of stopping power S(E) which is defined as the amount of energy lost over unit length of path of the particle in a given absorber, i.e;

$$S(E) = -\frac{dE}{dx} \tag{2.2.1}$$

2.2.4 Energy losses

COLLISION ENERGY LOSS:

The loss of energy from a charged particle to the surrounding medium by collision process has been studied by many workers, following the early calculation of Bohr, using classical theory. In particular Bethe, and Bloch, have evolved Quantum Mechanical treatments for both relativistic non-relativistic particles.

A particle of charge ze and velocity v=β c, passing through a material of atomic number Z, atomic weight A, and density ρ, will be presented with a total electron

cross-section $percm^2$ equal to;[3]

$$\sigma_e = \pi r_o^2 Z[cm^2]$$

The linear absorption coefficient for electrons will be;

$$\mu_e = \frac{\pi r_o^2 N_a \rho Z}{A}[cm^{-1}]$$

Where N_a is the Avogadro's number and r_o is the classical electron radius. It is convenient to use the numerical value $\pi r_o^2 N_a = 0.154$. The specific energy loss, under these conditions according to Bethe is given by;[3]

$$\frac{-dE}{dx} = 4\pi r_o^2 (\frac{N_a Z m c^2 z^2}{A\beta^2}) \left[\log(\frac{2mc^2\beta^2}{ZI(1-\beta^2)} - \beta^2) \right] \tag{2.2.2}$$

Replacing mc^2 by 0.511Mev, and $\pi r_o^2 N_a = 0.154$, the energy loss in Mev per gm/cm is;

$$\frac{-dE}{dx} = 0.314 \times (\frac{Zz^2}{A\beta^2}) \left[\log(\frac{2mc^2\beta^2}{ZI(1-\beta^2)} - \beta^2) \right] \tag{2.2.3}$$

Where I is an excitation potential per electron, expressed in the above formula in Mev, is derived from a summation of various electron transitions of the atom, and is very approximately $I = 11.5 \times 10^{-6}[Mev]$.

The Bethe formula for non-relativistic particle of mass M becomes

$$\frac{-dE}{dx} = \frac{2\pi e^4 N_a Z z^2 M}{AEm} \log(\frac{4mE}{MZI}) \tag{2.2.4}$$

The specific energy loss of electrons differs somewhat from that of heavy particles owing to the identity of mass between two components of the system. Again Bloch, has given the following form for the rate of energy loss by electrons of energy E, in which only collisions resulting in a loss of less than T are considered; is given by;[5].

$$(\frac{-dE}{dx})_{ion} = (4\pi) r_o^2 (\frac{N_a Z m c^2}{A\beta^2}) \left[\log(\frac{Tmc^2\beta^2}{ZI(1-\beta^2)} - (1-\beta^2)/2) \right] \tag{2.2.5}$$

The total energy loss will result when T=E/2, which is the maximum energy that an electron can communicate to another electron in one collision. The effective range of an electron is markedly modified by the high degree of scattering experienced by the particle, and a beam of electrons suffers a roughly exponential absorption, with an end point depending on the initial energy. Positrons are scattered differently from electrons, but the ranges are roughly equal for equal initial energy in Aluminium. In materials of high Z, however, positrons have greater range.

RADIATIVE ENERGY LOSS(BREMSSTRAHLUNG):

The deceleration forces on a singly charged particle are a function of particle velocity, βc, and atomic density n in the surrounding matter. The deceleration is inversely proportional to the particle mass M and is proportional to the atomic number Z, of the atoms close to which it passes. From the classical considerations, the energy radiated is proportional to Z^2/M^2 and the specific energy loss is;[3]

$$\frac{-dE}{dx} = 2.5 \times 10^{-26}(\frac{nZ^2mE_o}{M^2c^2})[Mev/cm] \tag{2.2.6}$$

Where $E_o = Mc^2/(1-\beta^2)^{-1/2}$.

For electrons;

$$\frac{-dE}{dx} = nE_o\sigma_{rad}[Mev/cm] \tag{2.2.7}$$

Where σ_{rad} is cross-section for radiative loss-according to the calculations of Born's Approximation, is given by;[1]

$$\begin{aligned} \sigma_{rad} &= (16/3)\sigma' \\ \sigma_{rad} &= 4(\log(2E/mc^2) - 1/3)\sigma' \end{aligned}$$

For non-relativistic region and extreme relativistic region, respectively. Where $\sigma' = Z^2 r_o^2/137 = 5.71 \times 10^{-28} Z^2 [cm^2]$. The second equation for cross-section, which shows that the ratio of energy radiated to the initial energy increases logarithmically with the particle energy E, is true if screening of nuclear charge can be neglected. On the other hand, for complete screening of the nuclear charge it becomes;

$$\sigma_{rad} = \sigma' \big[4 \log(183 Z^{-1/3}) + 2/9 \big] \tag{2.2.8}$$

And σ_{rad} is constant.The description due to FERMI is illustrating. Defining $-(d\overline{E})_{rad}$ as the total average energy loss per path length dx he showed;

$$-(d\overline{E})_{rad} = -4Z^2 (nEr_o^2/137) \ln(183/Z^{1/3}) dx \tag{2.2.9}$$

Where $E = h\nu_{max}$ is the energy of incident electron. This form readily allows introduction of the concept of Radiation Length (ℓ_R). Thus if we define;

$$\ell_R = 1/4Z^2 (nr_o^2/137) \ln(183/Z^{1/3}) \tag{2.2.10}$$

Then $-(d\overline{E})_{rad} = -(E/\ell_R)dx$ or $E = E_o \exp(-x/\ell_R)$. Hence, for $x = \ell_R$, the particle energy falls to 1/2.7 of its original value. For practical purposes the total energy loss per unit path length of the electron is the sum of ionization and radiative loss.i.e;

$$(\frac{dE}{dx})_{total} = (\frac{dE}{dx})_{ion} + (\frac{dE}{dx})_{rad} \tag{2.2.11}$$

The empirical relation;

$$\frac{(\frac{dE}{dx})_{rad}}{(\frac{dE}{dX})_{ion}} = \frac{EZ}{800} \tag{2.2.12}$$

is found to be approximately true where E is electron energy in Mev and Z is the atomic number of the absorber.

Chapter 3

Absorbed dose in NaI(Tl) scintillation detector

INTRODUCTION

Absorbed Dose(D): of any Ionizing Radiation is the energy imparted to matter by ionizing particles per unit mass of irradiated material, at the point of interest.

The problem at hand:

To measure/calculate the absorbed dose of a given radioactive point source in NaI(Tl) scintillator crystal of known efficiency.

The method to attack the problem:

Here we apply the scintillation detector for absorbed dose measurement at different thicknesses as well as the absorbed dose in the whole crystal, based on;

1. The interaction coefficients discussed in chapter two.

2. The counting data from the response function produced by NaI(Tl) scintillation detector for mono-energetic gamma-ray point radioactive source.

One important property of a detector in the application of radiation spectroscopy can be examined by noting its response function, (the differential pulse-height distribution

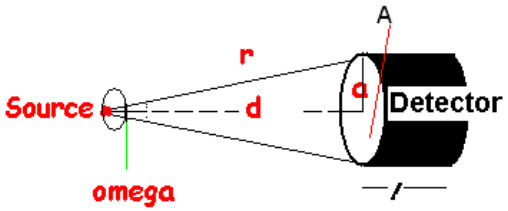

Figure 3.1: The solid angle Ω subtended by the detector at the source point

produced by a detector for the energy used in the determination).

3.1 Composition and geometrical relations

The response function to be expected for a real gamma-ray detector will depend on: the shape, size, and the composition of the detector, and also on the geometric details of the irradiation conditions.

3.1.1 Source-detector geometry

Suppose a radioactive point source emitting $N_{\gamma e}$, number or radiation quanta per second is located at a distance d from the aperture of a cylindrical detector of known efficiency as shown in the fig. 3.1 .

Where omega represent the solid angle (in steradian) subtended by the detector at the source position. The solid angle is defined by an integral over the detector surface that faces the source as;

$$\Omega = \int_A \frac{\cos(\alpha) dA}{r^2} \tag{3.1.1}$$

Where r represent the distance between the source and the surface element dA, and α is the angle between the normal to the surface element and the source direction. If the volume of the source is not negligible(i.e not a point source), then a second integration must be carried out over all the volume elements of the source. For our case of a point source located at the axis of a right circular cylindrical detector, the solid, Ω can be obtained from the fractional solid angle Ω_f as follows;

$$\begin{aligned} \Omega_f &= \frac{1}{4\pi}\int_A d\Omega \\ \Omega_f &= \frac{1}{4\pi}\int_0^{2\pi}\int_0^{\theta}\sin\theta d\theta \\ \Omega_f &= \frac{1}{2}[1-\frac{d}{\sqrt{a^2+d^2}}] \\ \Omega &= 4\pi\times\Omega_f \end{aligned} \tag{3.1.2}$$

Hence, the solid angle can be calculated from;

$$\Omega = 2\pi[1-\frac{d}{\sqrt{a^2+d^2}}] \tag{3.1.3}$$

3.1.2 Crystal shape, size and composition

CRYSTAL SHAPE: Two general crystal shapes are in widespread use for applications in gamma-ray detection;

The solid right circular cylinder :Two points are important

- If the height-to-diameter ratio of the cylinder does not greatly exceed unity, the collection properties are quite favorable in this geometry.
- If the height-to-diameter ratio is much less than one the pulse height resolution can often be improved by interposing the light pipe between the

cylinder and the photomultiplier tube to spread the light more uniformly from each scintillation event over the entire photocathode and thereby average out special variations of its quantum efficiency.

A well crystal :Is a right circular cylinder into which a cylindrical well has been machined usually along the cylindrical axis. A significant advantage of this geometry is the very high counting efficiency that can be achieved by placing the samples to be counted at the bottom of the well. In this position, almost all the gamma rays that are emitted isotropically from the source are intercepted by at least a portion of the crystal.

- For low energy gamma-rays, the counting efficiency in this geometry can approach 100percent.
- At higher energies, some of the advantage is lost, because the average path length through the crystal is somewhat less than if the gamma-rays were externally incident on a solid crystal. Because the efficiency for the source near the bottom of the well is not a sensitive function of position.

The composition and geometric conditions for the problem we set, can be summarized as follows;

SHAPE AND SIZE : We choose a solid cylindrical NaI(Tl) detector of size 7.62cm $\times$ 7.62cm.

COMPOSITION : For 0.001 mole-fraction of Thallium concentration as an activator material, the density of the detector is $\rho = 3.67[g/cm^3]$, the mean atomic number Z=64, atomic weight A=150 and the number of atoms per unit volume n=1.47412 $\times 10^{22}[atm/cm^3]$.

IRRADIATION CONDITION : Suppose a solid cylindrical 7.62cm by 7.62cm NaI(Tl) scintillation crystal is irradiated by mono-energetic gamma-rays of energy E_γ=1.369Mev emitted from (^{24}Na) point radioactive source, which is placed at d=10cm axial distance as shown in the fig. 3.1 . From the above considerations we want to calculate the absorbed dose in the crystal in the following sections.

3.2 Dosimetric quantities

To calculate the absorbed dose, and other dosimetric quantities in a NaI(Tl) scintillator material first we need to define the basic radiation field quantities, because absorbed dose in various materials are obtained from the product of radiation field quantities and some of the energy dependent interaction coefficients.

3.2.1 Radiation field quantities

Source of ionizing radiation may be characterized by its rate of emission of ionizing particles, and give rise to a Radiation Field. Within this field there will be Fluence, defined as

Fluence(Φ) = dN/da , Is the number of particles (dN) incident on a sphere of cross-section da.

Energy Fluence(Ψ) = dR/da , Is the radiant energy(dR) entering a sphere of cross-section da.

Differentiating w.r.t time we get fluence rate ($\phi = d\Phi/dt$) and the energy fluence rate ($\psi = d\Psi/dt$). There are distributions in direction and energy of fluence and energy fluence. Distribution in direction is the distribution of radiation in space, and it can be measured by a collimated detector that only accepts radiation that is coming from a limited solid angle. Also that the response of a detector to a particular particle fluence is frequently a function of the energy distribution, thus we define differential distributions as;

Differential distribution of fluence of particles : with respect to energy is ($d\Phi_E = \Phi_E dE$).

The total fluence with energies lying between E and E+dE is ;

$$\Phi = \int_0^{E_{max}} \Phi_E dE \tag{3.2.1}$$

Differential distribution of energy fluence : with respect to energy is ($d\Psi_E = \Psi_E dE$)

The total energy fluence with energies lying between E and E+dE is;

$$\Psi = \int_0^{E_{max}} \Psi_E dE \tag{3.2.2}$$

Mean or"effective" Energy:

Mean Energy(E_f) : of the particle weighted by fluence is;

$$E_f = \frac{\int_0^{E_{max}} E\Phi_E dE}{\int_0^{E_{max}} \Phi_E dE} \tag{3.2.3}$$

Mean Energy(E_e) : weighted by energy fluence is;

$$E_e = \frac{\int_0^{E_{max}} E\Psi_E dE}{\int_0^{E_{max}} \Psi_E dE} \tag{3.2.4}$$

3.2.2 Definitions of Absorbed Dose(D), Kerma(K) and Exposure(X)

The process of energy absorption is important even if, latter followed by complex physical, chemical and biological processes. However, to determine the energy absorbed by the irradiated materials is usually taken as a step in obtaining a quantitative correlation between the radiation and the effect it produces. Hence, we give a quantitative definitions as;

Absorbed dose(D) : The absorbed dose of any ionizing radiation is the energy imparted to matter by ionizing radiation per unit mass of the irradiated material at the point of interest, defined by;

$$D = \frac{d\varepsilon}{dm} \tag{3.2.5}$$

where $d\varepsilon$ is the mean energy imparted by the ionizing radiation to material of mass dm.

Kerma(K) : Kerma is the acronym for kinetic energy released per unit mass, it was introduced to emphasize the two stage process that takes place when indirectly ionizing particles such as photons or neutrons impart energy to matter. In the first stage the uncharged particles transfer their energy to the kinetic energy of the charged particles. In the second stage those charged particles impart energy to matter(in the sense used in the definition of absorbed dose), it is defined by;

$$K = \frac{dE_{tr}}{dm} \tag{3.2.6}$$

where dE_{tr} is the initial kinetic energy of all the charged ionizing particles in a

material of mass dm. It also includes the energy of those charged particles later radiate in bremsstrahlung.

Exposure(X) : Is the ratio of dQ by dm, where dQ is the absolute value of the total charge of the ions of one sign produced in air when all the electrons(negatrons and positrons) librated by photons in air of mass dm are complectly stopped in air, thus it is defined by;

$$X = \frac{dQ}{dm} \tag{3.2.7}$$

This definition requires two restrictions:

- The only material to enter into the chain of interactions is Air.
- Any ionization caused by the subsequent reabsorption of the bremsstrahlung is not to be included.

RELATIONS WITH FLUENCE AND ENERGY FLUENCE

The relations of fluence (Φ) and energy fluence (Ψ) with the dosimetric quantities D, K and X can be summarized for uncharged ionizing particles as;

$$\Psi = \frac{D}{(\frac{\mu_{en}}{\rho})_m} \tag{3.2.8}$$

Where the above equation holds under condition of charged particle equilibrium.

$$\Psi = \frac{K}{(\frac{\mu_{tr}}{\rho})_m} \tag{3.2.9}$$

$$\Psi = \frac{X(W_{air}/e)}{(\frac{\mu_{tr}}{\rho})_{air}} \tag{3.2.10}$$

The last equation holds for photons only, where W_{air} is the mean energy required to produce an ion pair in air. And $(\frac{\mu_{en}}{\rho})_m$ and $(\frac{\mu_{tr}}{\rho})_m$ are the mass energy absorption and mass energy transfer coefficients, of the detector material, respectively. The two coefficients are related by;

$$\frac{\mu_{en}}{\rho} = \frac{\mu_{tr}}{\rho}(1-g) \tag{3.2.11}$$

Where g is a fraction of the kinetic energy of the charged particles that is converted to photon energy escaped from the material(bremsstrahlung). And this fraction can be appreciable at high energies, specially in materials of high atomic number.

The interaction coefficients vary with the particle energy. If the particles have the range of energies, the coefficients used must be weighted according to the spectral distribution of energy fluence with respect to energy. In all cases the fluence can be obtained from the relationship between fluence and energy fluence, namely;

$$\Phi = \frac{\Psi}{\overline{E}} \tag{3.2.12}$$

Where $\overline{E} = E_f$ is the mean particle energy weighted by fluence. However, if the particles are mono-energetic and the fluence or flux is mono-directional, then the interaction coefficient is related to the fractional attenuation of fluence by

$$\Phi_\ell/\Phi_o = \exp(-\mu.m/\rho) \tag{3.2.13}$$

Where Φ_ℓ and Φ_o are the initial fluence and the fluence after traversing the thickness ℓ of the material respectively. And $m = \rho.\ell$ [gm/cm^2] as defined earlier in chapter two is the mass thickness of the material of density $\rho[gm/cm_3]$.

3.2.3 Units of measurements

Originally rad as the unit of absorbed dose was defined as: "A dose of radiation which spent 100 ergs of energy per gram." Now the SI unit gray(Gy)=(1J/Kg) is a recommended unit of absorbed dose, kerma, specific energy and absorbed dose index. As there are four quantities that can be expressed in gray, it is necessary to state what quantity is involved when a number of grays is mentioned unless this is clear from the context. Furthermore, as absorbed dose, kerma and specific energy can apply to any material, a statement of absorbed dose...etc is incomplete without an indication of the material concerned.

RELATIONS AMONG UNITS

Roentgen(r) : Is defined as a dose of gamma-ray or X-ray which produces in dry air, having a volume of one milliliter at 0 degree Celsius and 760mm of pressure 1e.s.u of charge (+ve or -ve) due to ionization.

- To express in terms of (C/Kg). Since one milliliter of dry air at zero degree Celsius and 760mm pressure has a mass of 0.001293gm

$$\begin{aligned} 1e.s.u &= 1/3 \times 10^{-9}[C] \\ 1r &= 1e.s.u/0.001293[gm] \\ 1r &= (10^{-9}/3)/(1.293 \times 10^{-6})[C/Kg] \\ 1r &= 2.58 \times 10^{-4}[C/Kg] \end{aligned}$$

- Since each singly charged ion carries $1.6 \times 10^{-19}C$ of charge and the energy needed to produce one ion pair in air is 32.5ev, and also $1ev = 1.6 \times 10^{-19}$

[J]

$$\begin{aligned} 1r &= \frac{10^{-9}}{3 \times 1.6 \times 10^{-19}} \times \frac{32.5 \times 1.6 \times 10^{-19}}{1.293 \times 10^{-6}} \\ 1r &= 83.8 \times 10^{-4}[J/Kg] \\ 1r &= 83.8 \times 10^{-4}[Gy] \\ 1r &= 83.8[ergs/gm] \end{aligned} \tag{3.2.14}$$

Thus, we have the following relations;

$$1Gy = 1J/Kg = 10^4[ergs/gm] = 100rad = 3.08 \times 10^{-2}[C/Kg]$$

Another unit of interest is to measure the source activity is curie(Ci).

Curie(Ci) : Is defined as exactly 3.7×10^{10} disintegrations/second, which owes its definition to its origin as the best available estimate of the activity of pure^{226}Ra. Later replaced by its SI equivalent, the Becquerel(Bq), where $1Bq = 2.703 \times 10^{-11}$ [Ci].

3.3 Derivation of the mathematical expressions

We first derive the fluence and energy fluence for a point gamma-ray source situated along the axis of a cylindrical detector and then we apply it to the calculation of absorbed dose.

3.3.1 Fluence and energy fluence

Fluence and energy fluence are most readily measured in the case of collimated mono-directional beams of particles. This collimated beam is made to fall on a suitable

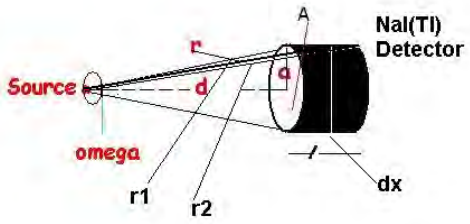

Figure 3.2: The solid angle Ω subtended by the detector at the source point

detector which has a known efficiency of detection for the radiation concerned. This efficiency of most detectors will be a function of the particles energy, therefore, interpretation of the results of detection require both the knowledge of this function and the energy distribution.

We want to apply this principle to calculate the emission rate of a point radioactive source and/or the fluence ($\Phi_{\gamma i}$) falling on the detector surface, as shown in the fig. 3.2 for the conditions defined at the end of section 3.2 .

where the solid angle Ω is as given in equation 3.1.3 .

DETECTION EFFICIENCY:

It is necessary to have a precise figure for the detection efficiency in order to relate the number of pulses counted to the number of photons incident on the detector, this is because of that not all the particles emitted from the source are entering the sensitive volume of the detector. On the other hand uncharged radiations such as gamma-rays or neutrons must first undergo a significant interactions in the detector before detection is possible. Therefore, it is convenient to subdivide counting efficiencies into two

classes:*absolute and intrinsic* efficiencies.

Absolute Efficiency : is defined as;

$$\epsilon_{abs} = \frac{number of pulses recorded}{number of radiation quanta emitted by source} \tag{3.3.1}$$

And they are dependent not only on the detector properties but also on the details of the counting geometry (primarily on the distance from the source to the detector).

The Intrinsic Efficiency: is defined as;

$$\epsilon_{int} = \frac{number of pulses recorded}{number of quanta incident on detector} \tag{3.3.2}$$

The two efficiencies are simply related for isotropic sources by;

$$\epsilon_{int} = \epsilon_{abs}(4\pi/\Omega) \tag{3.3.3}$$

A detector with a known efficiency can be used to measure the absolute activity and/or the emission rate of a radioactive source. we assume that a detector with an intrinsic efficiency of ϵ_{int} has been used to record N events under the full energy peak in the detector spectrum. For simplicity, we also assume that the source emits radiation isotropically , and no attenuation takes place between the source and the detector. From the definition of intrinsic peak efficiency, the number of radiation quanta $N_{\gamma e}$ emitted by the source over the measurement period can be determined from;

$$\epsilon_{abs} = \epsilon_{int}(\Omega/4\pi) \tag{3.3.4}$$

by substituting $\epsilon_{abs} = N/N_{\gamma e}$, and $\epsilon_{int} = N/N_{\gamma i}$ in equation 3.3.4 we get $N_{\gamma e}$ in terms

of $N_{\gamma i}$, the number of quanta incident on the detector as;

$$\begin{aligned} \epsilon_{abs} &= \epsilon_{int}(\Omega/4\pi) \\ \frac{N}{N_{\gamma e}} &= \frac{N}{N_{\gamma i}} \end{aligned} \tag{3.3.5}$$

$$N_{\gamma e} = N_{\gamma i}(4\pi/\Omega) \tag{3.3.6}$$

In the expression of intrinsic efficiency,($\epsilon_{int} = N/N_{\gamma i}$), if $N = N_{peak}$=peak area, then the efficiency is intrinsic peak efficiency (ϵ_{peak}) and, if $N = N_{tot}$=total area, that is the total area under the entire spectrum, then the intrinsic efficiency is called intrinsic total efficiency (ϵ_{tot}). Making these substitutions we get;

$$N_{\gamma e} = \frac{N_{peak}}{\epsilon_{peak}}(4\pi/\Omega) \tag{3.3.7}$$

The two efficiencies are related by the ratio known as the photofraction (peak-to total) ratio, defined as the ratio of the area under the full-energy-peak to that under the entire response function, given by;

$$p = \frac{\epsilon_{peak}}{\epsilon_{tot}} \tag{3.3.8}$$

Any measurement of absolute emission rates of gamma-rays(i.e not relative to a similar source of known activity) requires the knowledge of detection efficiency. The emission rate for a point source can then be calculated from the above equation by measuring or calculating, the full energy peak area and using tabulated data or graphs of sodium iodide detector efficiencies and by determining the solid angle from its dimensions: the thickness and the source-detector spacing. The following table lists

radionuclides used for efficiency calibrations, together with decay data necessary to compute gamma-ray yields from absolute activity.

Nuclide	$T_{1/2}$	E(Kev)	$I^a(perc)$	$\Delta I/I^b(perc)$
^{22}Na	2.60y	1274.5	99.95	0.0
^{24}Na	15.0h	1368.5	100.0	0.0
		2754.0	99.85	0.0
^{46}Sc	87.7d	889.2	99.98	0.0
		1120.5	99.99	0.0
^{54}Mn	312.5d	834.8	99.98	0.0
^{57}Co	272d	14.4	9.6	1.0
		122.1	85.6	0.3
^{60}Co	5.27y	1173.2	99.88	0.0
		1332.5	99.98	0.0
^{85}Sr	64.8d	13.4	50.7	1.5
		514.0	99.28	0.0
^{88}Y	106.6d	14.2	52.5	1.5
		1836.1	99.4	0.2
^{95}Nb	35.15d	765.8	99.80	0.0
^{113}Sn	115.2d	24.1	79.5	2.0
^{131}I	8.02d	364.5	82.4	0.5
^{134}Cs	2.06y	604.6	97.5	0.2
^{137}Cs	30.0y	31.8/32.6	5.64	2.0
		661.6	85.3	0.4
^{139}Ce	137.6d	33.0/33.4	64.1	2.0
		165.8	80.0	0.4
^{141}Ce	32.5d	35.6/36.0	12.6	2.0
		145.5	48.4	0.9
^{140}La	40.27h	1596.6	95.6	0.3
^{198}Au	2.696d	411.8	95.53	0.1
^{203}Hg	46.6d	70.8/72.9	10.1	1.5
		279.2	81.3	0.2
^{241} Am	432y	59.5	36.0	1.0

Table 3.1 Radionuclides used for efficiency calibrations,together with decay data necessary to compute gamma-ray yields from absolute activity

[a]I:Gamma-ray photon yield per disintegration [b]Δ I/I:Uncertainity in yield figure. Note:Only those gamma-ray lines are listed for which the yield uncertainty is 2.0percent or less. . Using the peak-to-total ratio (p=0.3 taken from graph of fig. 3.4 [2],[source:Debertin et al:64]), we can calculate the intrinsic peak efficiency of the detector for a given gamma-ray energy (E_γ), by;

$$\begin{aligned} p &= \frac{\epsilon_{peak}}{\epsilon_{tot}} \\ \Rightarrow \epsilon_{peak} &= p \times \epsilon_{tot} \end{aligned}$$

ϵ_{tot}, the intrinsic total efficiency is just the value of the gamma-ray interaction probability $(1 - \exp(-\mu\ell))$ integrated over all path length ℓ taken by those gamma-rays that strike the detector, can be obtained from;

$$\epsilon_{tot} = 2\int_0^{\ell} (1 - \exp(-\mu\ell'))d\ell' \tag{3.3.9}$$

To take account of all gamma-rays striking the detector at an angle θ above and below the axis of the detector let's consider fig. 3.3 .

For a=3.81cm and d=10cm;

$$\begin{aligned} \tan\theta &= \frac{a}{x+d} \\ \Rightarrow x &= a\cot\theta - d \\ \Rightarrow dx &= -a\csc^2\theta d\theta \\ at[x=0], \theta &= \tan^{-1}(a/d), \\ at[x=\ell], \theta &= \tan^{-1}(a/d+\ell), \\ \Rightarrow & \end{aligned}$$

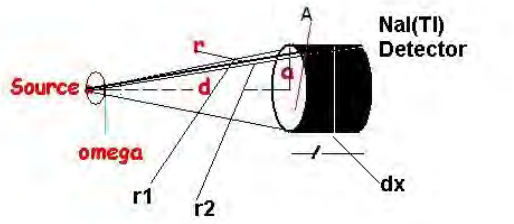

Figure 3.3: Source-detector geometry

θ =20.9 and 12.2, respectively. where $\mu = 0.221$, as calculated in subsection 3.3.2 is the linear total attenuation coefficient for the gamma-ray interactions given by;

$$\mu = n(\sigma_c + \sigma_p + \sigma_{pr})[cm^{-1}] \tag{3.3.10}$$

And n is the number of atoms per unit volume of the detector material, i.e $n = N_a\rho/M$, where ρ and M are the density and gram molecular weight of the detector. Then ϵ_{tot} is;

$$\begin{aligned}
\epsilon_{tot} &= 2\int_0^{\ell}(1-\exp(-\mu\ell'))d\ell' \\
\epsilon_{tot} &= (-2a)\int_{\theta=20.9}^{\theta=12.2}(1-\exp(-\mu(a\cot\theta - d)))\csc^2\theta d\theta \\
\epsilon_{tot} &= (2a/\mu)bigg[\mu(\cot\theta_2 - \cot\theta_1) + (\exp(-\mu(a\cot\theta_1 - d)) - \exp(-\mu(a\cot\theta_2 - d)))bigg] \\
\epsilon_{tot} &= 0.10443
\end{aligned}$$

The intrinsic peak efficiency is then; $\epsilon_{peak} = 0.3 \times \epsilon_{tot} = 0.031329$.

From the pulse height spectra of the mono-energetic gamma-ray of ^{24}Na, E_γ=1.369Mev measured experimentally by 3" $\times$ 3" NaI-Tl detector, the number of counts corresponding to the photo-peak is $N_{peak} = 8.139 \times 10^7$[CPS] [2].

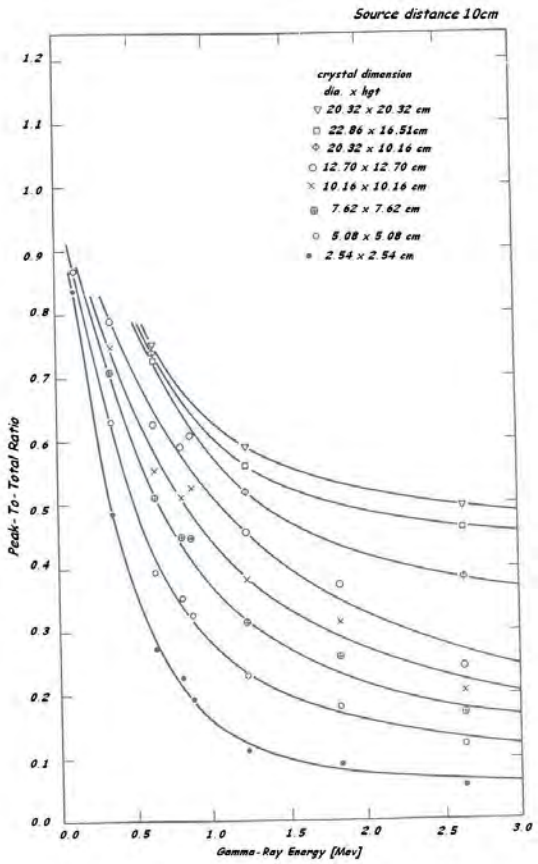

Figure 3.4: Peak-to-total ratio(or the photofraction) for various solid cylinders of NaI(Tl) for a point gamma ray source 10cm from the scintillator surface.(courtesy of Harshaw Chemical Company.)

Then the photon fluence ($\phi_{\gamma i}$), assuming the gamma-rays beam falling perpendicular to the aperture of circular area πa^2 is

$$\Phi_{\gamma i} = N_{\gamma i}/\pi a^2 \tag{3.3.11}$$

Then the energy fluence (Ψ_γ), for the average energy available per interaction, ($\overline{E}$) in the medium is given by;

$$\Psi_\gamma = \overline{E}\Phi_{\gamma i} \tag{3.3.12}$$

Where the average energy available per interaction in a coterminous medium, with complete multiple scattering is given by [3];

$$\overline{E} = (1/\sigma)\Big((\sigma_c + \sigma_p)E_\gamma + (E_\gamma - 1.02)\sigma_{pr}\Big) \tag{3.3.13}$$

3.3.2 Derivation of absorbed dose

There are two cases to be considered, absorbed dose with and without bremsstrahlung production.

WITHOUT BREMSSTRAHLUNG:

Suppose a parallel beam of high energy E_γ photon of energy fluence Ψ_γ falls normally on the aperture of a cylindrical detector, as illustrated in the fig. 3.5 .

If the beam is broad, then the energy fluence within the medium near the central axis will show no lateral variation and the energy fluence will decrease down the central axis with an effective linear attenuation coefficient μ. The compton recoil electrons(or any electron-positron pair) will tend to be ejected in the same direction as the photons producing them. In any event the gradient of the electron energy fluence will be zero, at right angle to the central axis of the bean. The electron energy fluence will be assumed to fall off axially with an effective linear attenuation coefficient μ_e. As the

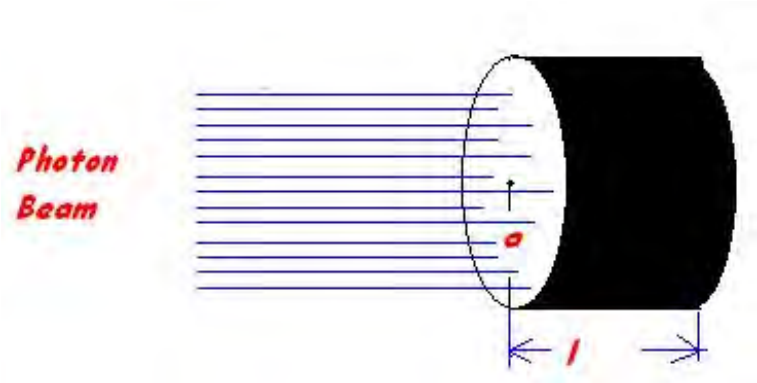

Figure 3.5: A parallel beam of photon falling on the aperture of circular cross-section

linear attenuation coefficient of the photons is μ, the photon energy fluence at a depth x will be;

$$\Psi_x = \Psi_\gamma \exp(-\mu x) \tag{3.3.14}$$

If μ_{tr} is the energy transfer coefficient of the medium for photons, then this will release an electron energy fluence in a thickness dx of the medium, Ψ_{ex} given by $\Psi_{ex} = \Psi_\gamma \mu_{tr} \exp(-\mu x) dx$. In traveling a greater distance x_1 the electron energy fluence will be attenuated by a factor $\exp(-\mu_e(x_1 - x))$, hence;

$$\begin{aligned} \frac{d\Psi_{ex1}}{\Psi_{ex}} &= \exp(-\mu_e(x_1 - x)) \\ \Rightarrow d\Psi_{ex1} &= \Psi_{ex} \exp(-\mu_e(x_1 - x)) \\ d\Psi_{ex1} &= \Psi_\gamma \mu_{tr} \exp(-\mu x) \exp(-\mu_e(x_1 - x)) dx \end{aligned}$$

Then the absorbed dose dD_{x1} in the volume of unit area, thickness, dx and density, ρ will be:

$$\begin{aligned} dD_{x1} &= (\mu_e/\rho) d\Psi_{ex1} \\ \Rightarrow D_{x1} &= (\mu_e/\rho) \int_0^{x1} d\Psi_{ex1} \end{aligned}$$

The absorbed dose at x1 is then given by:

$$\begin{aligned} D_{x1} &= \frac{\Psi_\gamma \mu_{tr} \mu_e}{\rho} \int_0^{x1} \exp(-\mu x) \exp(-\mu_e(x_1 - x)) dx \\ \Rightarrow D_{x1} &= \frac{\Psi_\gamma \mu_{tr} \mu_e}{\rho(\mu_e - \mu)} \Big[\exp(-\mu x1) - \exp(-\mu_e x1) \Big] \end{aligned}$$

Since, $\Psi_\gamma = \overline{E}\Phi_{\gamma i}$;

$$D_{x1} = \frac{\overline{E}\Phi_{\gamma i} \mu_{tr} \mu_e}{\rho(\mu_e - \mu)} \Big[\exp(-\mu x1) - \exp(-\mu_e x1) \Big] \tag{3.3.15}$$

KERMA(K_x):The kerma at x1 can be calculated from; $\Psi_x = \Psi_\gamma \exp(-\mu x1)$:

$$\begin{aligned} K_{x1} &= (\frac{\mu_{tr}}{\rho})\Psi_x \\ K_{x1} &= (\frac{\mu_{tr}}{\rho})\Psi_\gamma \exp(-\mu x1) \end{aligned}$$

The kerma at any point x in the detector can be calculated from;

$$K_x = \overline{E}\Phi_{\gamma i}(\frac{\mu_{tr}}{\rho}) \exp(-\mu x) \tag{3.3.16}$$

WITH BREMSSTRAHLUNG PRODUCTION:

μ'_e must be substituted for μ_e in the absorbed dose equation, hence the absorbed dose D_{x2} will be:

$$D_{x2} = \frac{\overline{E}\Psi_\gamma \mu_{tr} \mu'_e}{\rho(\mu'_e - \mu)} \Big[\exp(-\mu x) - \exp(-\mu'_e x) \Big] \tag{3.3.17}$$

Where μ'_e is that part of μ_e that arises from radiative collision energy loss, this means that, the absorbed dose is reduced by a factor (μ'_e/μ_e) everywhere.

With no attenuation of photons ($\mu = 0$), the absorbed dose (D_x) would be;

$$D_x = \overline{E}\Phi_{\gamma i} \frac{\mu_{tr}}{\rho} \Big[1 - \exp(-\mu_e x) \Big] \tag{3.3.18}$$

These are the final formulae with which we calculate the absorbed dose and kerma, at various x_i depthes.

For the numerical calculation, the following parameters should be specified first for a gamma-ray energy $E_\gamma = 1.369 Mev$;

Mean Energy : $\overline{E} = (1/\sigma)\Big[(\sigma_c + \sigma_p)E_\gamma + (E_\gamma - 1.02)\sigma_{pr}\Big]$

Linear Absorption And Transfer Coefficients : If $\mu_{tr} and \mu$, are the linear transfer coefficient and absorption coefficient, these can be calculated, respectively, as;

$$\begin{aligned}(\mu_{tr}/\rho) &= (n/\rho)\Big[\sigma_p(1-\delta/h\nu) + \sigma_c + \sigma_{pr}(1 - 2m_o c^2/h\nu)\Big] \\ \mu_{tr} &= 0.220[percm]\end{aligned}$$

Where, $\delta = 5.5ev$ delta-rays emitted for NaI(Tl).

$$\begin{aligned}\mu &= n.(\sigma_c + \sigma_p + \sigma_{pr}) \\ \mu &= 1.47412 \times 10^{22}(11.8968 + 3.043 + 0.027841) \times 10^{-24}[1/cm] \\ \mu &= 0.221[cm^{-1}]\end{aligned}$$

Where $n = \frac{N_a \rho}{A}$ is the number of atoms per unit volume, ρ=3.67[g/cm^3] is the density and A=150 is the mean gram molecular weight of the detector material(NaI-Tl). Hence; $n = 1.47412 \times 10^{22}[atoms/cm^3]$. Each of the cross-sections for the three major photon interactions in the detector medium can be calculated as;

- The compton cross-section is:

$$\begin{aligned}\sigma_c &= 0.2E^{-1/2}Z, where Z = 64 \\ \Rightarrow \sigma_c &= 0.2(1.1576Mev)^{-1/2} \times 64 \\ \sigma_c &= 11.8968 \times 10^{-24}[cm^2]\end{aligned}$$

And E is the kinetic energy for the maximum emission in the forward direction;

- The photoelectric cross-sections are: $\sigma_p = 3 \times 10^{-9} E^{-7/2} \times Z^5$[barn] and $\sigma_p = 3.8 \times 10^{-9} E^{-1} \times Z^5$[barn], for low energy and high energy gamma-rays,respectively.

  The cross-section for photoelectric process for high energy gamma-ray is;

$$\begin{aligned} \sigma_p &= 3.8 \times 10^{-9} \times (1.341)^{-1}.(64)^5 \\ \sigma_p &= 3.043 \times 10^{-24}[cm^2] \end{aligned}$$

- The cross-section for pair production:

$$\begin{aligned} \sigma_{pr} &= 6.2 \times 10^{-5}(E - 1.02)^{2.1} \times Z^2[barn] \\ \Rightarrow \sigma_{pr} &= 6.2 \times 10^{-5}(1.369 - 1.02)^{2.1} \times (64)^2 \\ \sigma_{pr} &= 0.027841 \times 10^{-24}[cm^2] \end{aligned}$$

Where E in all of the cases is the kinetic energy of the secondary electrons given by;

- For the photoelectric interaction; $E = E_\gamma - E_b[Mev]$,

$$\begin{aligned} E &= E_\gamma - E_b \\ E &= (1.369 - 0.028)[Mev] \\ E &= 1.341 Mev \end{aligned}$$

  where $E_b = 0.028 Mev$ is the binding energy of the electron in the K-shell for the iodine atom in NaI(Tl).

- For the pair production; $E = (E_\gamma - 1.02)[Mev] ... for E_\gamma \geq 1.02 Mev$

$$\begin{aligned} E &= (E_\gamma - 1.02)[Mev] \\ E &= 0.349 Mev \end{aligned}$$

- For the compton process in which the maximum emission of electrons in the forward direction;

$$\begin{aligned} E &= \frac{4E_\gamma^2}{(1+4E_\gamma)} \\ E &= 4(1.369)^2/1 + 4 \times 1.369 \\ E &= 1.1576[Mev] \end{aligned}$$

The Linear Attenuation Coefficient For Electrons :

- with no bremsstrahlung is given by;

$$\begin{aligned} \mu_e &= \pi r_o^2 N_a (\frac{\rho Z}{A}) \\ \Rightarrow \mu_e &= 0.154(\rho Z/A) \\ \mu_e &= \frac{0.154 \times 3.67 \times 64}{150} \\ \mu_e &= 0.2411[percm] \end{aligned}$$

- With bremsstrahlung production is;

$$\begin{aligned} \mu_e' &= n.\sigma_{rad} \\ \sigma_{rad} &= 4(\log(\frac{2E}{mc^2}) - 1/3)\sigma' \\ E &= \overline{E} - 0.511 Mev = 0.8561 Mev \\ \sigma' &= 5.71 \times 10^{-28} Z^2 \\ \mu_e' &= n.\sigma_{rad} = 0.026451[cm^{-1}] \end{aligned}$$

where E in the above expression is the particle energy.

3.4 Numerical calculation of fluence, energy fluence and absorbed dose

Fluence and energy fluence:

For d=10cm and a=3.81cm, the solid angle Ω subtended by the circular aperture of the detector at the location of the source can be calculated as;

$$\begin{aligned}
\Omega &= 2\pi[1 - \frac{d}{\sqrt{a^2 + d^2}}] \\
\Omega &= 2\pi(1 - \frac{10}{\sqrt{100 + 14.5161}}) \\
\Omega &= 2\pi(1 - 0.9345) \\
\Omega &= 0.412
\end{aligned}$$

To calculate the fluence, first we need to calculate the absolute emission rate of the source using;

$$N_{\gamma e} = (N_{peak}/\epsilon_{peak})(\frac{4\pi}{\Omega}) \tag{3.4.1}$$

The intrinsic peak efficiency is then;$\epsilon_{peak} = 0.3 \times \epsilon_{tot} = 0.031329$. From the pulse height spectra of the mono-energetic gamma-ray of ^{24}Na, E_γ=1.369Mev measured experimentally by 3" $\times$ 3" NaI-Tl detector as shown in the fig.3.6, the number of counts corresponding to the photo-peak is $N = 8.139 \times 10^7$[CPS]. Substituting all the above calculated values we get the absolute emission rate of the source as;

$$\begin{aligned}
N_{\gamma e} &= (N_{peak}/\epsilon_{peak})(\frac{4\pi}{\Omega}) \\
N_{\gamma e} &= \frac{8.139 \times 10^7}{0.031329}(\frac{4\pi}{\Omega}) \\
N_{\gamma e} &= 7.924 \times 10^{10}[dis]
\end{aligned}$$

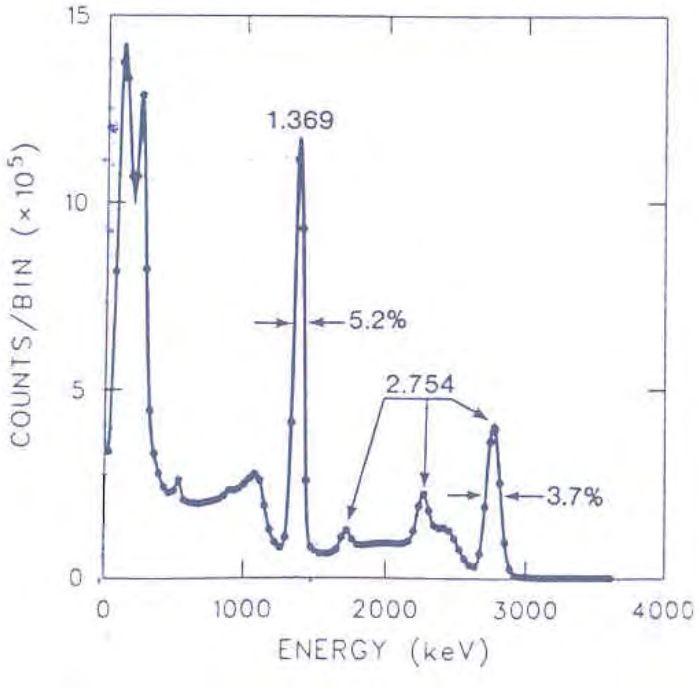

Figure 3.6: Comparative Pulse Height Spectra Measured By 7.62cm by 7.62cm NaI(Tl) Scintillator For Gamma-Rays From ^{24}Na.From Moss et al

With no attenuation between the source and the detector, fluence falling perpendicular to the circular aperture of the detector will be.

$$\Phi_{\gamma i} = 5.697 \times 10^7 [dis/cm^2] \tag{3.4.2}$$

Because from the tabulated data: "Decay data for radionuclides used as efficiency standard", given in table 3.1, we can see that-the gamma-ray photon yield per disintegration for ^{24}Na is 100 percent. This means we get one photon yield per disintegration, therefore, the fluence incident on the surface is;

$$\Phi_{\gamma i} = 5.697 \times 10^7 [photons/cm^2] \tag{3.4.3}$$

Dose Calculation :Using the formula for the average energy available per interaction of a gamma-ray in a coterminous medium, $\overline{E}$, with complete multiple scattering we calculate Ψ_γ, where $\overline{E}$ is given by;

$$\overline{E} = (1/\sigma)\Big[(\sigma_c + \sigma_p)E_\gamma + (E_\gamma - 1.02)\sigma_{pr}\Big] \tag{3.4.4}$$

Substituting the cross-sections we get $\overline{E} = 1.3671 Mev/photons$. Then the photon energy fluence is;

$$\begin{aligned} \Psi_\gamma &= \overline{E}\Phi_{\gamma i} \\ \Psi_\gamma &= 1.3671 \times 5.697 \times 10^7 [photons/cm^2] \\ \Psi_\gamma &= 7.7884 \times 10^7 [Mev/cm^2] \end{aligned}$$

Using this energy fluence in the absorbed dose formula derived earlier, we can calculate the dose at various depthes of the crystal. With no bremsstrahlung production the

absorbed dose D_{x1} at x depth is;

$$D_{x1} = \frac{\Psi_\gamma \mu_{tr} \mu_e}{\rho(\mu_e - \mu)} \Big[\exp(-\mu x) - \exp(-\mu_e x) \Big] \tag{3.4.5}$$

$$\begin{aligned} D_{x1} &= \frac{7.7884 \times 0.220 \times 0.2411 \times 10^7}{3.67(0.2411 - 0.221)} \Big[\exp(-\mu x) - \exp(-\mu_e x) \Big] \\ D_{x1} &= 5.60023 \times 10^7 \Big[\exp(-\mu x) - \exp(-\mu_e x) \Big] [Mev/g] \\ D_{x1} &= 0.0089604 \Big[\exp(-\mu x) - \exp(-\mu_e x) \Big] [Gy] \end{aligned}$$

Kerma can also be calculated by using;

$$K_x = \frac{\Psi_\gamma \mu_{tr}}{\rho} \exp(-\mu x) \tag{3.4.6}$$

Substituting the values of transfer coefficient and energy fluence ;

$$\begin{aligned} \mu_{tr} &= 0.220[cm^{-1}] \\ \Psi_\gamma &= 7.7884 \times 10^7 [Mev/cm^2] \end{aligned}$$

The Kerma at various depthes can be calculated by using;

$$K_x = 0.00074701 \times \exp(-\mu x)[Gy] \tag{3.4.7}$$

For the case of bremsstrahlung production, the absorbed dose can be calculated by using;

$$D_{x2} = \frac{\Psi_\gamma \mu_{tr} \mu'_e}{\rho(\mu'_e - \mu)} \Big[\exp(-\mu x) - \exp(-\mu'_e x) \Big] \tag{3.4.8}$$

Therefore, in the presence of bremsstrahlung, the absorbed dose at various depthes can be calculated from;

$$\begin{aligned} D_{x2} &= \frac{7.7884 \times 0.220 \times 0.026451 \times 10^7}{3.67(0.2411 - 0.221)} \Big[\exp(-\mu x) - \exp(-\mu'_e x) \Big] \\ D_{x2} &= 0.00098304 \times \Big[\exp(-\mu x) - \exp(-\mu'_e x) \Big] [Gy] \end{aligned}$$

With no attenuation of photons, the Absorbed Dose (D_x) would be;

$$\begin{aligned} D_x &= \overline{E}\Psi_\gamma \frac{\mu_{tr}}{\rho} \Big[1 - \exp(-\mu_e x) \Big] \\ D_x &= 0.00074701 \Big[1 - \exp(-\mu_e x) \Big] [Gy] \end{aligned}$$

DATA ANALYSIS AND INTERPRETATION OF RESULT

for the calculation of absorbed dose and kerma at various depthes of a 3"by 3"NaI-Tl scintillator crystal:

By dividing the thickness ℓ into N=100 equal subintervals, we calculate kerma (K_x), and the absorbed doses; D_x, D_{x1} and D_{x2}, respectively, using the equations;

1. $K_x = 0.00074701 \times \exp(-\mu x)[Gy]$
2. $D_x = 0.00074701 \Big[1 - \exp(-\mu_e x) \Big] [Gy]$...with no photon attenuation.
3. $D_{x1} = D_{x1} = 0.0089604 \Big[\exp(-\mu x) - \exp(-\mu_e x) \Big] [Gy]$...without Bremsstrahlung.
4. $D_{x2} = 0.00098304 \times \Big[\exp(-\mu x) - \exp(-\mu'_e x) \Big] [Gy]$

And we get the result as tabulated below, from table 3.3 up to 3.7.

$x[cm]$	$D_{x1}[Gy]$	$K_x[Gy]$	$D_x[Gy]$	$D_{x2}[Gy]$
0.000000E+00	0.000000E+00	7.470100E-04	0.000000E+00	0.000000E+00
7.620000E-02	1.348447E-05	7.345355E-04	1.359864E-05	1.479367E-06
1.524000E-01	2.649818E-05	7.222694E-04	2.694972E-05	2.907100E-06
2.286000E-01	3.905388E-05	7.102080E-04	4.005778E-05	484550E-0.26
3.048000E-01	5.116284E-05	6.983482E-04	5.292718E-05	5.613039E-06
3.810000E-01	6.283763E-05	6.866863E-04	6.556234E-05	6.893857E-06
4.572000E-01	7.408931E-05	6.752192E-04	7.796748E-05	8.128264E-06
5.334000E-01	8.492859E-05	6.639436E-04	9.014674E-05	9.317489E-06
6.096000E-01	9.536774E-05	6.528563E-04	1.021044E-04	1.046274E-05
6.858000E-01	1.054166E-04	6.419541E-04	1.138443E-04	1.156518E-05
7.620000E-01	1.150857E-04	6.312340E-04	1.253705E-04	1.262596E-05
8.382000E-01	1.243850E-04	6.206929E-04	1.366869E-04	1.364620E-05
9.144000E-01	1.333251E-04	6.103278E-04	1.477973E-04	1.462700E-05
9.906000E-01	1.419151E-04	6.001358E-04	1.587054E-04	1.556941E-05
1.066800	1.501646E-04	5.901140E-04	1.694149E-04	1.647448E-05
1.143000	1.580833E-04	5.802596E-04	1.799295E-04	1.734323E-05
1.219200	1.656799E-04	5.705697E-04	1.902527E-04	1.817665E-05
1.295400	1.729637E-04	5.610417E-04	2.003880E-04	1.897571E-05
1.371600	1.799422E-04	5.516727E-04	2.103387E-04	1.974135E-05
1.447800	1.866247E-04	5.424602E-04	2.201083E-04	2.047450E-05
1.524000	1.930194E-04	5.334016E-04	2.297001E-04	2.117607E-05

Table 3.3 Values of D_{x1},K_x,D_x and D_{x2} at various depth of NaI-Tl crystal,with N=100 equal divisions

$x[cm]$	$D_{x1}[Gy]$	$K_x[Gy]$	$D_x[Gy]$	$D_{x2}[Gy]$
1.600200	1.991345E-04	5.244942E-04	2.391172E-04	2.184692E-05
1.676400	2.049771E-04	5.157356E-04	2.483630E-04	2.248791E-05
1.752600	2.105553E-04	5.071232E-04	2.574404E-04	2.309989E-05
1.828800	2.158766E-04	4.986547E-04	2.663526E-04	2.368368E-05
1.905000	2.209480E-04	4.903275E-04	2.751025E-04	2.424007E-05
1.981200	2.257770E-04	4.821394E-04	2.836931E-04	2.476984E-05
2.057400	2.303701E-04	4.740881E-04	2.921274E-04	2.527375E-05
2.133600	2.347342E-04	4.661712E-04	3.004081E-04	2.575254E-05
2.209800	2.388757E-04	4.583866E-04	3.085381E-04	2.620694E-05
2.286000	2.428018E-04	4.507318E-04	3.165200E-04	2.663764E-05
2.362200	2.465180E-04	4.432050E-04	3.243567E-04	2.704535E-05
2.438400	2.500307E-04	4.358038E-04	3.320507E-04	2.743073E-05
2.514600	2.533461E-04	4.285263E-04	3.396047E-04	2.779444E-05
2.590800	2.564696E-04	4.213702E-04	3.470212E-04	2.813712E-05
2.667000	2.594071E-04	4.143337E-04	3.543026E-04	2.845938E-05
2.743200	2.621641E-04	4.074146E-04	3.614515E-04	2.876184E-05
2.819400	2.647460E-04	4.006111E-04	3.684702E-04	2.904510E-05
2.895600	2.671578E-04	3.939212E-04	3.753612E-04	2.930972E-05
2.971800	2.694051E-04	3.873431E-04	3.821267E-04	2.955628E-05
3.048000	2.714929E-04	3.808747E-04	3.887691E-04	2.978532E-05
3.124200	2.734260E-04	3.745144E-04	3.952905E-04	2.999739E-05

Table 3.4 Values of D_{x1},K_x,D_x and D_{x2} at various depth of NaI-Tl crystal,with N=100 equal divisions

$x[cm]$	$D_{x1}[Gy]$	$K_x[Gy]$	$D_x[Gy]$	$D_{x2}[Gy]$
3.200400	2.752089E-04	3.682603E-04	4.016933E-04	3.019300E-05
3.276600	2.768464E-04	3.621107E-04	4.079794E-04	3.037266E-05
3.352800	2.783434E-04	3.560637E-04	4.141512E-04	3.053687E-05
3.429000	2.797036E-04	3.501177E-04	4.202106E-04	3.068612E-05
3.505200	2.809319E-04	3.442711E-04	4.261596E-04	3.082087E-05
3.581400	2.820325E-04	3.385220E-04	4.320004E-04	3.094160E-05
3.657600	2.830089E-04	3.328690E-04	4.377349E-04	3.104873E-05
3.733800	2.838656E-04	3.273103E-04	4.433650E-04	3.114273E-05
3.810000	2.846065E-04	3.218445E-04	4.488926E-04	3.122401E-05
3.886200	2.852353E-04	3.164700E-04	4.543195E-04	3.129298E-05
3.962400	2.857555E-04	3.111852E-04	4.596477E-04	3.135005E-05
4.038600	2.861706E-04	3.059887E-04	4.648788E-04	3.139562E-05
4.114800	2.864847E-04	3.008789E-04	4.700148E-04	3.143006E-05
4.191000	2.867006E-04	2.958544E-04	4.750572E-04	3.145376E-05
4.267200	2.868221E-04	2.909139E-04	4.800078E-04	3.146708E-05
4.343400	2.868521E-04	2.860559E-04	4.848684E-04	3.147038E-05
4.419600	2.867940E-04	2.812790E-04	4.896405E-04	3.146399E-05
4.495800	2.866505E-04	2.765818E-04	4.943256E-04	3.144825E-05
4.572000	2.864249E-04	2.719632E-04	4.989255E-04	3.142350E-05
4.648200	2.861200E-04	2.674216E-04	5.034417E-04	3.139006E-05
4.724400	2.857387E-04	2.629558E-04	5.078756E-04	3.134823E-05

Table 3.5 Values of D_{x1},K_x,D_x and D_{x2} at various depth of NaI-Tl crystal,with N=100 equal divisions

$x[cm]$	$D_{x1}[Gy]$	$K_x[Gy]$	$D_x[Gy]$	$D_{x2}[Gy]$
4.800600	2.852839E-04	2.585647E-04	5.122288E-04	3.129832E-05
4.876800	2.847580E-04	2.542469E-04	5.165028E-04	3.124062E-05
4.953000	2.841637E-04	2.500011E-04	5.206990E-04	3.117542E-05
5.029200	2.835036E-04	2.458263E-04	5.248188E-04	3.110300E-05
5.105400	2.827802E-04	2.417212E-04	5.288636E-04	3.102363E-05
5.181600	2.819956E-04	2.376847E-04	5.328347E-04	3.093757E-05
5.257800	2.811527E-04	2.337155E-04	5.367336E-04	3.084509E-05
5.334000	2.802533E-04	2.298127E-04	5.405615E-04	3.074643E-05
5.410200	2.793001E-04	2.259750E-04	5.443197E-04	3.064183E-05
5.486400	2.782948E-04	2.222014E-04	5.480095E-04	3.053154E-05
5.562600	2.772396E-04	2.184908E-04	5.516321E-04	3.041579E-05
5.638800	2.761368E-04	2.148422E-04	5.551887E-04	3.029480E-05
5.715000	2.749882E-04	2.112545E-04	5.586807E-04	3.016878E-05
5.791200	2.737956E-04	2.077267E-04	5.621091E-04	3.003795E-05
5.867400	2.725611E-04	2.042579E-04	5.654750E-04	2.990251E-05
5.943600	2.712865E-04	2.008469E-04	5.687797E-04	2.976267E-05
6.019800	2.699735E-04	1.974929E-04	5.720242E-04	2.961862E-05
6.096000	2.686239E-04	1.941949E-04	5.752097E-04	2.947056E-05
6.172200	2.672393E-04	1.909520E-04	5.783371E-04	2.931865E-05
6.248400	2.658213E-04	1.877633E-04	5.814077E-04	2.916309E-05

Table 3.6 Values of D_{x1},K_x,D_x and D_{x2} at various depth of NaI-Tl crystal,with N=100 equal divisions

$x[cm]$	$D_{x1}[Gy]$	$K_x[Gy]$	$D_x[Gy]$	$D_{x2}[Gy]$
6.324600	2.643716E-04	1.846278E-04	5.844223E-04	2.900405E-05
6.400800	2.628917E-04	1.815447E-04	5.873821E-04	2.884169E-05
6.477000	2.613831E-04	1.785130E-04	5.902880E-04	2.867618E-05
6.553200	2.598472E-04	1.755320E-04	5.931410E-04	2.850768E-05
6.629400	2.582856E-04	1.726007E-04	5.959420E-04	2.833635E-05
6.705600	2.566994E-04	1.697185E-04	5.986920E-04	2.816233E-05
6.781800	2.550900E-04	1.668843E-04	6.013920E-04	2.798576E-05
6.858000	2.534588E-04	1.640975E-04	6.040429E-04	2.780680E-05
6.934200	2.518069E-04	1.613572E-04	6.066455E-04	2.762558E-05
7.010400	2.501358E-04	1.586626E-04	6.092007E-04	2.744223E-05
7.086600	2.484462E-04	1.560131E-04	6.117094E-04	2.725689E-05
7.162800	2.467397E-04	1.534078E-04	6.141724E-04	2.706967E-05
7.239000	2.450173E-04	1.508460E-04	6.165906E-04	2.688069E-05
7.315200	2.432799E-04	1.483270E-04	6.189647E-04	2.669009E-05
7.391400	2.415286E-04	1.458500E-04	6.212957E-04	2.649796E-05
7.467600	2.397646E-04	1.434145E-04	6.235842E-04	2.630443E-05
7.543800	2.379888E-04	1.410196E-04	6.258311E-04	2.610960E-05

Table 3.7 Values of D_{x1},K_x,D_x and D_{x2} at various depth of NaI-Tl crystal,with N=100 equal divisions

When the four plotted together we get the following curves as shown in the fig.

3.7 . INTERPRETATION OF RESULT

The absorbed dose and kerma obtained from this direct approach are position sensitive, therefore, it can be used as a good representative for the spatial distribution of the scintillation lights generated by the interaction of gamma-ray(emitted by the radioisotope) with the detector medium.

To find a particular depth x-at which $D_{x1} = K_x$, we divide the expression obtained

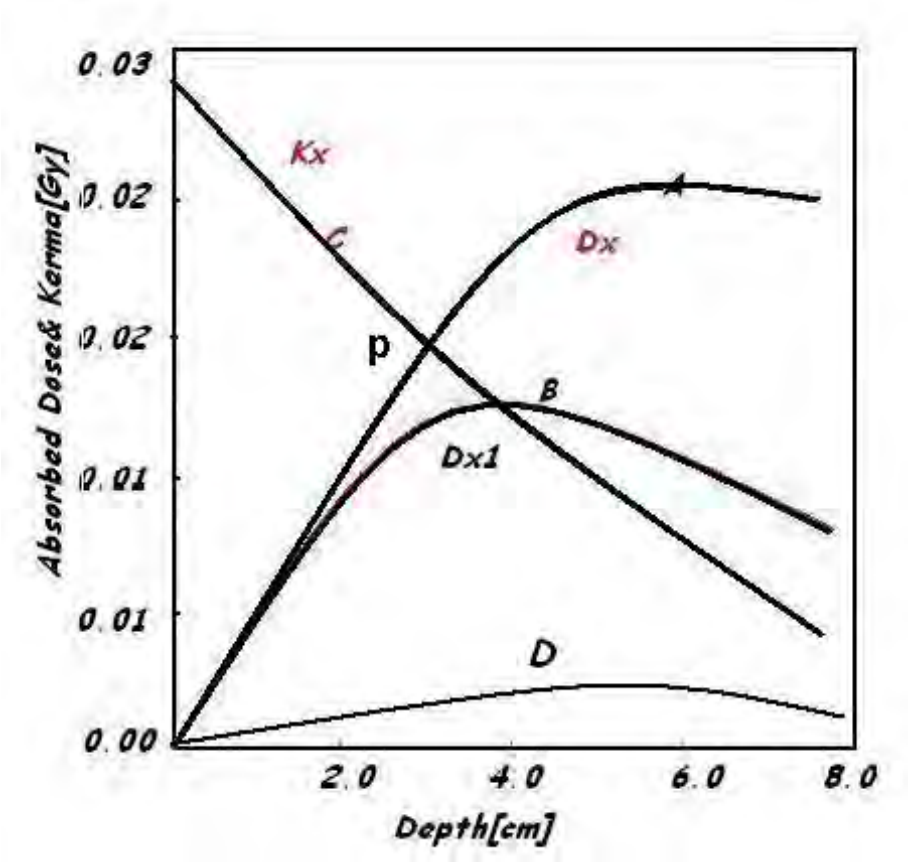

Figure 3.7: Absorbed dose and kerma Curves: A is absorbed dose if no attenuation of primary photons, B with no bremsstrahlung, C is kerma and D is actual absorbed dose:,.

for absorbed dose by the expression of kerma:

$$\frac{D_{x1}}{K_x} = \frac{\mu_e}{(\mu_e - \mu)}[1 - \exp(-(\mu_e - \mu)x)] \tag{3.4.9}$$

If $D_{x1} = K_x$, then $x = \ln(\mu_e/\mu)/(\mu_e - \mu)$. When x is large enough to make the exponential term negligible the above ratio reduces to $\frac{D_{x1}}{K_x} = \frac{\mu_e}{(\mu_e - \mu)}$. This shows that the absorbed dose and kerma bear a constant ratio to one another, with the absorbed dose being greater.

Mean Energy Range : It can be shown that on the falling part of the absorbed dose and kerma $D_x = K_x - d$, that is, if $\mu_e \gg \mu$, then $d = 1/\mu_e$. This means, in the exponential attenuation, the attenuation coefficient is the reciprocal of the mean energy range of the attenuated particles, therefore, $d = 1/\mu_e$ is the mean range of the secondary electrons.

Intersection Point : The point of intersection (p) of dose and kerma, on the graph can be calculated as;

$$\begin{aligned} x &= \frac{\ln(\mu_e/\mu)}{(\mu_e - \mu)} \\ x &= \frac{\ln(0.235/0.216)}{(0.235 - 0.216)} \\ x &= 4.437[cm], where \\ D_{x1} &= 0.4211[Gy] and \\ K_x &= 0.4210[Gy] \end{aligned}$$

It may also be shown that, at a point where kerma and absorbed dose curves intersect the primary radiation has been attenuated by the factor(f) given by;

$$f = \frac{\mu/\mu_e \ln(\mu_e/\mu)}{(1 - \mu/\mu_e)} \tag{3.4.10}$$

f=0.95711

The energy deposited in the whole crystal can be calculated from the absorbed dose with bremsstrahlung, because this interaction is a significant process for the particle energy greater than 1Mev, hence

$$\begin{aligned} D_c &= \frac{dE_t}{dm} \\ \Rightarrow E_t &= \int D_c dm \\ E_t &= (\pi a^2 \rho) \int_0^{\ell} D_c dx \end{aligned}$$

where $D_c = D_{x2}$, and this implies that;

$$E_t = (\pi a^2) \frac{\Psi_\gamma \mu_{tr} \mu'_e}{(\mu'_e - \mu)} \times \int_0^{\ell} \exp(-\mu x) - \exp(-\mu_e x) dx \tag{3.4.11}$$

The integration will result;

$$E_t = (\pi a^2) \frac{\Psi_\gamma \mu_{tr} \mu'_e}{(\mu'_e - \mu)} \times \left[\frac{\exp(-\mu'_e x - 1)}{\mu'_e} - \frac{\exp(-\mu x - 1)}{\mu} \right] \tag{3.4.12}$$

Substituting all the necessary values in the above expression we get;

$E_t = 2.034535 \times 10^7$[Mev]

The actual dose rate is then obtained by dividing the above result by the mass of the detector, i.e, m=ρ v=1275.2 gm, and hence we get;

$$\begin{aligned} D_c &= \frac{E_t}{m} \\ D_c &= 1.595463 \times 10^5 [Mev/gm] \\ D_c &= 1.595463 \times 10^5 \times 1.6 \times 10^{-10} [Gy] \\ D_c &= 0.000025527 [Gy] \end{aligned}$$

The total energy deposited without bremsstrahlung production can be determined by integrating the absorbed dose D_{x1}, in the whole volume of the crystal as;

$$\begin{aligned} D_c &= \frac{dE_t}{dm} \\ \Rightarrow E_t &= \int D_c dm \\ E_t &= (\pi a^2 \rho) \int_0^{\ell} D_c dx \end{aligned}$$

where $D_c = D_{x1}$, and this will give E_t to be;

$$E_t = (\pi a^2) \frac{\Psi_\gamma \mu_{tr} \mu_e}{(\mu_e - \mu)} \times \int_0^{\ell} \exp(-\mu x) - \exp(-\mu_e x) dx \tag{3.4.13}$$

The integration will result;

$$E_t = (\pi a^2) \frac{\Psi_\gamma \mu_{tr} \mu_e}{(\mu_e - \mu)} \times \left[\frac{\exp(-\mu_e x - 1)}{\mu_e} - \frac{\exp(-\mu x - 1)}{\mu} \right] \tag{3.4.14}$$

$E_t = 1.854471756 \times 10^9$[Mev]

The absorbed dose is then obtained by dividing the above result by the mass of the detector, i.e, m=ρ v=1275.2 gm, and hence we get;

$$\begin{aligned} D_{cw} &= \frac{E_t}{m} \\ D_{cw} &= 1.454259 \times 10^6 [Mev/gm] \\ D_{cw} &= 1.454259 \times 10^6 \times 1.6 \times 10^{-10} [Gy] \\ D_{cw} &= 0.000232681 [Gy] \end{aligned}$$

Taking the ratio of absorbed dose without to with bremsstrahlung we get the factor by which the actual absorbed dose is increased. That is;

$$\frac{D_{cw}}{D_c} = 0.000232681/0.000025527$$
$$\frac{D_{cw}}{D_c} = 9.115$$

This could also be deduced from;

$$\frac{\mu_e}{\mu'_e} = 0.2411/0.026451$$
$$\frac{\mu_e}{\mu'_e} = 9.115$$

3.5 Conclusion and summary

The absorbed dose calculated above employs an analytic method, which is based on the recorded data; the peak count rate corresponding to the peak-efficiency and the pulse height distribution produced by NaI(Tl) scintillation counter for the mono-energetic gamma-ray point source, ^{24}Na.

Most scintillation counting is carried out in a pulse mode operation. And the output of a detector operated in a pulse mode normally consists of a string of individual signal pulses, each representing the interaction of a single quantum of radiation within the detector. Measurement of the rate at which such pulses occur will give the corresponding rate of radiation interaction within the detector.

If the number of fluorescent quanta (scintillations) emitted and the number of photoelectrons released from the cathode by these scintillations can be made to be proportional to the energy expended by the gamma radiation that is incident on the detector material, as stipulated in the introductory chapter, then the scintillation

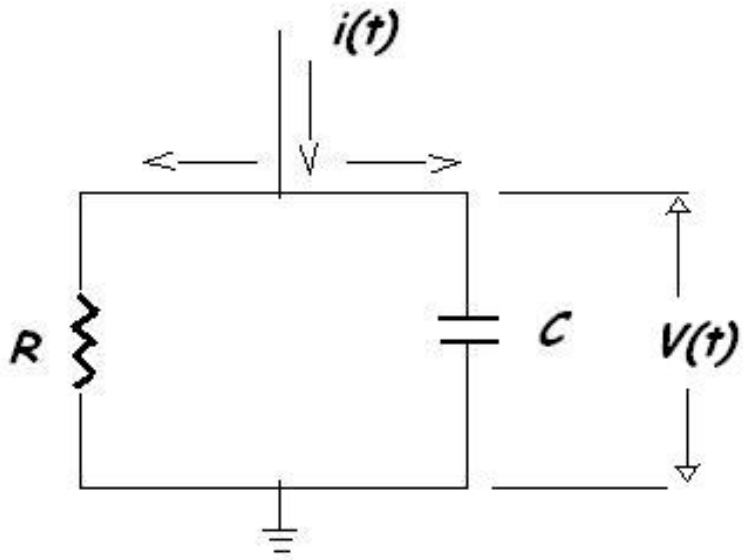

Figure 3.8: Simple parallel RC circuit representing a PM tube anode circuit.

detector can be used to produce impulsive charge of magnitude Q proportional to the energy dissipated by the incident radiation and hence to the absorbed dose.
To make this comparison let's consider the voltage pulse at the anode of the PM tube following a scintillation event, which is dependent on the time constant of the anode circuit, idealized by fig.3.8 .

The current flowing in the anode i(t) is simply the current of electrons from a single pulse, assumed to be at t=0. The principal component of the emitted light from most scintillation detectors can be adequately represented as a simple exponential decay. Since the current is given by;

$$i(t) = i_o \exp(-\lambda t) \tag{3.5.1}$$

Where $\lambda = 1/\tau_d$ is the scintillation decay constant and the initial current i_o can

be expressed in terms of the total charge Q collected over the entire pulse by noting;

$$\begin{aligned} Q &= \int_0^\infty i(t)dt \\ Q &= \int_0^\infty \exp(-\lambda t)dt \\ Q &= i_o/\lambda \end{aligned}$$

Therefore, $i(t) = \lambda Q \exp(-\lambda t)$. But $i(t) = i_c + i_R$. Then writing the the capacitor and the resistor currents in terms of their respective voltages we get the following first order differential equation.

$$\frac{dV(t)}{dt} + \frac{1}{RC}V(t) = \frac{\lambda Q}{C}\exp(-\lambda t) \tag{3.5.2}$$

With the initial condition V(0)=0 the solution cab be expressed as;

$$V(t) = \frac{1}{\lambda - Q} \times \frac{\lambda Q}{C}[\exp(-\theta t) - \exp(-\lambda t)] \tag{3.5.3}$$

Where $\theta = 1/RC = 1/\tau$ is the reciprocal of the anode time constant.
At high counting rate applications the anode time constant is made large compared with the scintillation decay time τ_d, that is, $\theta \gg \lambda$, and hence;

$$V(t) \cong \frac{Q}{C}[\exp(-\theta t) - \exp(-\lambda t)] \tag{3.5.4}$$

We can split the voltage into two cases;

1. If t is much greater than the scintillation decay time, then long time approximation for the voltage will be;

$$V(t) \cong (Q/C)\exp(-\theta t) \tag{3.5.5}$$

2. If t is much less than the anode time constant, then short time approximation for the voltage will be;

$$V(t) \cong (Q/C)[1 - \exp(-\lambda t)] \tag{3.5.6}$$

The following generalities will hold true for a wide variety of radiation detectors, operated under the condition in which $\tau = RC \gg \tau_d$.

- The leading edge is detector dependent and the trailing edge is circuit dependent.
- The amplitude of the signal pulse is determined simply by the ratio of the total charge Q created within the detector during one radiation interaction divided by the capacitance C, of the equivalent load circuit.

Because this capacitance is normally fixed, the amplitude of signal pulse is directly proportional to the corresponding charge generated within the detector and, hence;

$$V_{max} = Q/C \tag{3.5.7}$$

But this is reached only if $\theta \ll \lambda or \tau \gg \tau_d$. The experimenter, thus must choose a time constant that is, at least 5-10 times greater than the scintillation decay time but this is not excessively long to prevent needless pulse pileup with the tail from a preceding pulse at high counting rates.

3.5.1 Validity

LIGHT OUTPUT:

A small fraction of the kinetic energy lost by a charged particle in a scintillator

is converted into fluorescent energy. The fraction of the particle energy which is converted (the scintillation efficiency) depends on both the particle type and the particle energy. In some cases, the scintillation efficiency may be independent of the particle energy. The response of a scintillator can best be described by a relation between (dL/dx), the fluorescent energy emitted per unit path length and the specific energy loss for the charged particle, (dE/dx). In the absence of quenching (radiationless transitions), the light yield is proportional to energy loss. That is;

$$\frac{dL}{dx} = s\frac{dE}{dx} \tag{3.5.8}$$

When detectors are excited by fast electrons (either directly or from gamma-ray irradiation), the above expression can be written as;

$$\frac{dL}{dx}|_e = s\frac{dE}{dx} \tag{3.5.9}$$

Or incremental light output per unit energy loss is a constant known as the scintillation efficiency of the detector, $dL/dE|_e = s$.

$\Rightarrow dL = sdE$, this shows that the light output is linearly related to the energy dissipated. In our case, if $L_1 = sE_1$, where $E_1 = E_d = 2.034535 \times 10^8 Mev$ and $L_2 = sE_2$, where $E_2 = E'_d = 1.854471756 \times 10^9 Mev$, we get the ratio $L_2/L_1 = 9.115$, which is exactly same as that obtained from the absorbed dose ratio and can be compared with that obtained experimentally in the conclusion part.

CONCLUSION

In NaI(Tl) detector, in addition to the prompt yield a phosphorescence with characteristic delay time of 15 sec. has also been measured which contribute about 9 percent to the overall light yield[17]. Other longer-lived phosphorescence components have also been measured[18]. This is because of that the dominant decay time of the

scintillation pulse from NaI(Tl) is 230nsec., unconformably long for some fast/high counting rates in which the anode time constant $\tau = RC << \tau_d$(decay time of the scintillator). Therefore, at high counting rates, the phosphorescence tend to build up due to the multiple overlap from many preceding pulses. This afterglow is often undesirable characteristic of sodium iodide used in high counting applications. Hence, the measured dose D_m, should be corrected for this contribution. That is;

$$\begin{aligned} D_m &= (1/9)D_{cw} \\ D_m &= (1/9)(0.000232681) \\ D_m &= 0.000025853[Gy] \end{aligned}$$

Since, $D_c = (1/9.115)D_{cw} = 0.000025527[Gy]$, the error can be calculated from;

$$\begin{aligned} Error &= |\frac{Meas.val - cal.val}{meas.val}| \times 100 percent \\ Error &= |\frac{D_m - D_c}{D_m}| \times 100 percent \\ Error &= |\frac{0.000025853 - 0.000025527}{0.000025853}| \times 100 percent \\ Error &= 1.26 percent \end{aligned}$$

SUMMARY

- The absorbed dose should be a reasonable measure of the chemical and physical effects created by a given radiation exposure in an absorbing material.
- In general the response function to be expected for a real gamma-ray detector

will depend upon, the shape, size, composition of the detector, and also on the geometric details of the irradiation condition.

- The calculated value of absorbed dose by the direct approach in this project work can only be achieved in practical measurement, if the NaI(Tl) crystal is well coupled to the PM tube together with its electronic assembly. But it can be used to get a rough estimates of the contribution from delayed phosphorescence to the overall light yield of the detector after setting the geometric conditions for a given type of gamma-ray.

- The most generally useful scintillator for gamma-ray detection is NaI(Tl), which can be obtained in the form of large clear crystals ranging in diameter from a few millimeter to 20cm, with a cylindrical shape. And the most generally useful size being from 4 to 10cm.

- The variation of thallium concentration above 0.1 percent(as an activator), has little effect on W-value, that large crystals should be capable of giving good energy resolution when properly coupled to a suitable PM tube. However, cautions should be exercised for the following conditions that may affect the energy resolution while setting the detector size;

1. The absorption of fluorescence light in the crystal increases the amplitude spread, particularly as the size of the phosphor is increased.

2. Non-uniformity in photosensitivity or collection efficiency over the surface of PM tube may also give rise to amplitude dispersion, unless light from the scintillating medium is more or less uniformly spread over the cathode. Where the

scintillator thickness is more than half the phosphor diameter, this condition is reasonably well fulfilled; otherwise, a short light guide of perspex may be interposed.

Bibliography

[1] CURRAN, F.R.S *Luminescence and the scintillation Counters*, London:Better Worth, 1964.

[2] Glenn, F. Knoll *Radiation Detection And Measurement*, John Wiley and Sons, 1989.

[3] J.sharpe *Nuclear Radiation Detectors*, London:Methuen and Co,LTD , 1964.

[4] SINGRU, R. M. *Introduction to Experimental Nuclear Physics* Cmbridge, Wiley Eastern Private LTD(New Delhi),1974.

[5] Bloch *Bloch,Quoted inHeitler ibid*,219.

[6] Fermi.E *"Nucl. Physics"*, Chicago, 1950.

[7] Katz And Penfold *Phys.Rev.,83,932*: 1951.

[8] Spring, *Photons And Elecrons, p-76*, Methuen, 1950.

[9] Heitler, *The Quntum Theory Of Radiation*, Oxford,2nd Edition, 1944.

[10] Gerbes, *Ann.Phys*,Leipzig,1935.

[11] V.perez-Menez, J.Monel, S.N.Kaplan, and R.A.Str *Nucl.Instrum.A252,478*, Meth, 1986.

[12] Bethesa ,MD. *NCRP Report No.58*, NCRP,1985.

[13] H.M.Weiss: *Nucl.Instrum,112,291*, Meth, 1973.

[14] Jalbert, R. A. and R.D.Hiebert, *Nucl.Instrum,96,61.* Meth. 1971.

[15] Bleuler and Zuntii. *Helt,phys,19,137*,Acta.,1946.

[16] Evans, R. D. *The Atomic Nucleus,p.717*, New York:Mc Graw-Hill Book Co.,Inc., 1955.

[17] M.salomon and S.S.A.Williams: *Nucl.instrum.A241,210*, Meth, 1985.

[18] H. Kume, S. Muramatsu, and M.Iida, IEEE Trans *Nucl.Science,NS(1),359*, 1986.